M 2021

U.PORTO
FEUP FACULDADE DE ENGENHARIA
UNIVERSIDADE DO PORTO

EFFECT OF THE AU LOADING ON THE PHOTOCATALYTIC HYDROGEN PRODUCTION FROM GLYCEROL OVER AU/TIO_2 CATALYSTS

BRUNO RIBEIRO
MASTER'S THESIS PRESENTED TO
FACULTY OF ENGINEERING OF UNIVERSITY OF PORTO IN
CHEMICAL ENGINEERING

Master in Chemical Engineering

Effect of the Au loading on the photocatalytic hydrogen production from glycerol over Au/TiO_2 catalysts

Master dissertation

of

Bruno Tiago Pereira Ribeiro

Developed within the course of dissertation

held in

LEPABE – Laboratory for Process Engineering, Environment, Biotechnology and Energy

Supervisor : **Doctor Miguel A. Soria**

Co-supervisors : **Doctor Carmen S.D. Rodrigues**

Professor Luís M. Madeira

July 2021

Acknowledgment

Firstly, I thank my Supervisor, Doctor Miguel Angel Soria and my two Co-Supervisors, Doctor Carmen S. Deus Rodrigues and Professor Doctor Luís Miguel Madeira, for the immense help, supervision, counseling and hospitality they have provided since the very beginning. I am also very grateful for the trust deposited in me, to develop this dissertation on this project, at LEPABE, to whom I am grateful.

To those who followed my work closely, my colleagues at the E-146 Laboratory, I am sincerely grateful, for making the duration of my dissertation at LEPABE a pleasure and a peaceful experience. To Catarina, Cristina, Joana, Salomé, Bruno, Pedro, Cláudio, but especially to Emanuel, Sandy, who puts up with me and my demons, in every situation, a big thank you, and it will not stop here.

To every single one of my friends, from MIEQ, FEUP, and *GGG*, I am deeply grateful for the daily reminder of what good friends are supposed to be. Every single day you help me through the rocky trail that is studying at FEUP, by standing by my side, living through most of the moments I will never forget. Thank you for all of these years of friendship, for everything.

To *Dragões*, the other parts of me, I am simply not able to express the amounts of gratitude and thankfulness I have for you. Each one of you shows me daily what love and friendship is, in its purest form, making everything, good, bad and in between, worth it. Thank you for holding me when I was falling, for crying with me, laughing with me, studying with me, partying with me, but above all, being with me. I am grateful for all that we lived, live and will continue to live. To you I truly owe my human being.

To my family, to every single person who either raised or was raised with me, thank you for all you've done for me. Thank you for always having a place to comfort me, I know I had it whenever I needed it. To you Dad, the reason I am who I am, I truly have no words capable of expressing the size of the gratefulness, love and affection I have for you. To you I owe everything. I am conquering the world because of you, because you love me. You make everything possible, even when you feel like you can't. Thank you for believing I could be someone in this world. Thank you for being there for me, when Mom couldn't. To you Mommy, thank you for helping me on the other side, I know you are watching me from up there, happy. To you I devote all of my love. One day I'll tell you everything I did in this life to make you and dad proud. I hope you saw it, I really did it for you. I miss you, in times like these I know you wanted to be here to hug me, and I wanted you here, so much. I dream of seeing you again.

Facing a global pandemic was not the ideal scenario to produce a dissertation, but the adversity only helped put pressure on myself to have a final product close to perfection. This work focuses

on a very new technology that is receiving exorbitant amounts of attention and focus, for the production of what is thought to be the future's energy vector, clean hydrogen.

Throughout the whole semester, I have put countless hours into research to help me understand the fundamentals of this process, helping me for the experimental work I had to conduct in the next phase and even before starting the experiments, I already had a firm idea of what I could do to improve this process.

Having to write a dissertation on my own helped me understand my limits and capacities, but it definitely made me develop very strong soft skills, which I consider to be the most valuable of this whole experience. I became much more focused and less of a procrastinator, I developed a sense of responsibility and work autonomy and became a better problem solver, which made me a better student, and I hope it will one day translate to both my professional and personal life.

Doctor Miguel A. Soria, supervisor and Doctor Carmen S.D. Rodrigues and Professor Luis M. Madeira, co-supervisors of this dissertation are integrated members of LEPABE – Laboratory for Process Engineering, Environment, Biotechnology and Energy, financially supported by: Base Funding - UIDB/00511/2020 of the Laboratory for Process Engineering, Environment, Biotechnology and Energy – LEPABE - funded by national funds through the FCT/MCTES (PIDDAC).

Abstract

Fossil fuels are now the most used energy source, currently being highly exploited to meet the energetic demand of the population worldwide. Furthermore, these high levels of fossil fuel exploration lead to extreme CO_2 emissions, which are probably the main responsible for global warming. Renewable energy sources are now rising to combat this problem by fossil fuel substitution, attenuating the greenhouse gas (GHG) emission, alleviating the future generations in terms of fuel consumption. From renewable sources arose the possibility of producing clean hydrogen by solar light harvesting, integrating waste streams of the biodiesel industry, mainly glycerol, in the photocatalytic hydrogen production process. Glycerol now stands as one of the focus points to produce clean H_2 by enhancing the biodiesel process at the economic and environmental levels simultaneously.

The most common photocatalysts used in this process is TiO_2 as a support for the deposition of other metals as co-catalysts, Au in this case. Several Au/TiO_2 photocatalysts were produced by deposition-precipitation technique, producing reliable and efficient catalysts for the hydrogen production. The photocatalytic experiments were conducted in a glass reactor (1 L), coupled with a Hg vapor lamp as the radiation source. In the experiments, the following variables were fixed: catalyst loading, 0.75 g L^{-1}; radiation intensity, 500 W m^{-2} and 0.3 L of a glycerol solution (5 vol.%). Optimization variables were then studied, namely, calcination pretreatment of the catalyst (Dried, 300—600 ºC), catalyst particle size (<100 and 100—200 µm), gold loading (1—4 wt. %), initial pH (5—10) and reaction temperature (50—90 ºC).

The best hydrogen productions came from a dried 3%Au/TiO_2 sample (uncalcined), with particle size of 100—200 µm, an initial pH of 6.38 and a reaction temperature of 90ºC, with a maximum rate of hydrogen production of 67 873 µmol g_{cat}^{-1} h^{-1}, totaling a final production, after 3 hours, of 155 119 µmol g_{cat}^{-1}. After optimal values were found, a long-test was performed to see the influence of the reaction duration, extending the total time to 26 hours, obtaining a maximum H_2 production rate of 52 753 µmol g_{cat}^{-1} h^{-1}, totaling a production of 668 263 µmol g_{cat}^{-1}. In this experiment, CO and CO_2 were also quantified, reaching a stable rate of production, after around 3 hours, of 546 and 2 290 µmol g_{cat}^{-1} h^{-1}, with production quantities of 41 345 and 169 836 µmol g_{cat}^{-1}, respectively.

The photocatalytic process was proven to be feasible in the studied range of parameters, with high efficiencies in terms of the hydrogen production, ascertaining to the possibility of employing glycerol (biodiesel waste streams) as a sacrificial agent to efficiently produce clean hydrogen.

Keywords: Photocatalysis; Hydrogen; TiO_2; Glycerol; Biodiesel

Resumo

Os combustíveis fósseis são a principal fonte de energia mundial, e estão atualmente a ser altamente explorados, em virtude das necessidades energéticas da população mundial. Esta exploração acentuada conduziu ao maior problema dos combustíveis fósseis, as elevadas emissões de CO_2, que é o maior responsável pelo aquecimento global. As energias renováveis estão agora a surgir como resposta a este problema, como substitutas, atenuando assim o problema das emissões de gases com efeito de estufa, assegurando as gerações futuras. Das renováveis nasceu a possibilidade de produzir hidrgénio limpo a partir da luz solar, integrando também resíduos da indústria do biodiesel, o glicerol, num processo de produção de hidrogénio a partir da fotocatálise. O glicerol é agora um foco mundial para a produção de hidrogénio, ajudando o processo a nível económico e ambiental.

Os fotocatalisadores mais empregues neste processo usam TiO_2 como suporte para a posterior deposição de outros metais como co-catalisadores, Au neste caso. Todos os fotocatalisadores de Au/TiO_2 foram preparados pelo método de deposição-precipitação, que produz catalisadores estáveis e eficientes. Os testes fotocatalíticos foram conduzidos num reator de vidro (1L), acoplado com um lâmpada de mercúrio como fonte de radiação. Nos testes realizados, foram fixadas as seguintes variáveis: concentração de glicerol, 5%vol., concentração de catalisador, 0,75 g L^{-1}; intensidade de radiação, 500 W m^{-2} e volume de solução, 0,3 L. As variáveis de otimização são nomeadamente a calcinação (seco, 300—600 ºC), tamanho de partícula (<100 e 100—200 µm), concentração de Au (1—4%), pH inicial (5—10) e temperatura de reação (50—90 ºC).

As melhores produções de hidrogénio foram observadas para o catalisador 3%Au/TiO_2, de tamanho 100—200 µm, com uma solução de glicerol com um pH de 6.38 a 90ºC, com um máximo na taxa de produção de 67 873 µmol g_{cat}^{-1} h^{-1}, totalizando uma produção total, depois de 3 horas, de 155 119 µmol g_{cat}^{-1}. Depois da otimização das variáveis, foi conduzido um teste de longa duração, de 26 horas, para ver a influência do tempo de reação, obtendo-se um máximo na produção de hidrogénio de 52 753 µmol g_{cat}^{-1} h^{-1}, finalizando o teste com uma produção total de hidrogénio de 668 263 µmol g_{cat}^{-1}. Neste teste também foram quantificados o CO_2 e CO formados durante a reação, totalizando uma produção de 41 345 e 169 836 µmol g_{cat}^{-1}, respetivamente, tendo estabilizado depois de três horas, em taxas de produção de 546 e 2 290 µmol g_{cat}^{-1} h^{-1}.

O processo de produção de hidrogénio por fotocatálise é, portanto, viável, nos valores das variáveis em estudo, com altas produções de hidrogénio e consequente eficiência do processo, que confirma a possibilidade de utilizar este processo para a valorização de resíduos do biodiesel, o glicerol, como reagentes sacrificiais para a produção de hidrogénio.

Palavras-chave: Fotocatálise; Hidrogénio; TiO_2; Glicerol; Biodiesel

Declaration

I hereby declare, under word of honor, that this work is original and that all non-original contributions is indicated and due reference is given to the author and source

July 5, 2021

Index

List of Figures

List of Tables

Notation and Glossary

[cat]	Catalyst concentration	g L^{-1}
$[glycerol]_0$	Initial glycerol concentration	g L^{-1}
Au^0	Metallic gold	
d_p	Particle diameter	μm
e^-_{CB}	Electron, in the Conduction Band	
h^+_{VB}	Hole, in the Valence Band	
I	Intensity (Lamp)	W m^{-2}
Vsol	Volume of solution	L

List of Acronyms

CB	Conduction Band
DP	Deposition-Precipitation
DPU	Deposition-Precipitation with Urea
FCEV	Fuel Cell Electric Vehicles
GHG	Greenhouse Gas
HT	Hydrothermal
IMP	Impregnation
LSPR	Localized Surface Plasmon Resonance
SG	Sol-Gel
VB	Valence Band
WIMP	Wet Impregnation

1 Introduction

Currently, fossil fuels are the main energy source for our society's energy consumption needs, given its maturity as a technology in the energy industry, encouraging their continuous use as a commodity. However, they are presently being highly exploited, depleting the amounts of resources yearly, creating a huge problem for future generations and putting pressure on world economies to start invest in the research of renewable energy sources to interrupt this extreme resource exploration. Moreover, fossil fuel utilization implies its combustion, contributing to the unavoidable production and emission of greenhouse carbon dioxide (CO_2), which is considered the main culprit of global warming.

This rampant rise in Greenhouse Gas (GHG) emissions over the last few decades will not stop, at least for the foreseeable future, as no downward trends are expected anytime soon. For reference, CO_2 emissions peaked in 2018, representing almost 75% of all GHG emissions, totaling around 33.2 Gt_{CO2}, evidenced by Figure 1 [1].

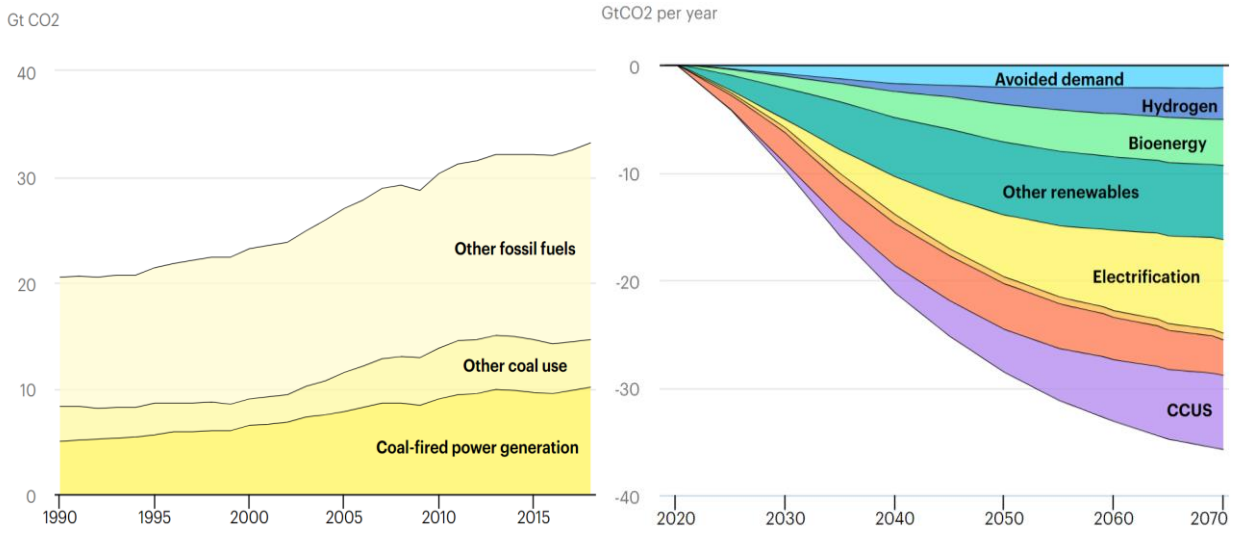

Figure 1 — (a) CO_2 emissions, by source, in Gt_{CO2}, and (b) CO_2 emission reduction estimation for the 2020-2070 period, in Gt_{CO2} $year^{-1}$. Retrieved from [2]

Therefore, the world needs to collectively and gradually reduce current GHG emissions as soon as possible. As a result, several plans and initiatives were established on climate change mitigation to prevent further damage and possibly provide long-term solutions, seen in Figure 1, through the sustainable forecast for the next 50 years. One of the main focus points is the substitution of non-renewable energy sources by environmentally friendlier alternatives: Renewable Energy Sources (RES).

Renewable energy sources are sustainable sources of energy that are regenerated at a sufficiently high rate so their depletion is not considerable. Nonetheless, renewable energy sources may not solve the problem on their own but are at least capable of alleviating it.

Indeed, renewables are now a big part of the energetic scenario of several countries, with a global 11.4% share of the total energy consumption, as of 2019 [1], with Portugal marking a 30.6% share of final energy consumption and a 53.6% share of final energy production from renewables, in 2020 [1] [3]. These values are still too weak to compete with fossil fuels, but forecasts are promising. Within these sources emerged what is considered the most promising energy solution yet, clean hydrogen. This simple yet powerful molecule can be the key to a future carbon-neutral society.

1.1 Hydrogen — The Energy of the Future

Clean hydrogen is currently experiencing unprecedented momentum as a rising technology, emerging as a plausible clean and safe energetic solution to the ongoing energetic problems. Due to its outstanding properties as an energy vector, it is able to convert and store energy, to then release it, so that electricity can be generated, so employing hydrogen as an energy carrier is an extremely beneficial path to a green society. Although promising, hydrogen is yet to be a clean source, as it is predominantly produced by carbonizing methods. In a hypothetic scenario, H_2 can decrease the energy dependence of a country, which indicates the extent to which an economy relies on importation of energy to meet their needs, given by the ratio between the net imports and the total gross available energy [4].

From a scientific point of view, hydrogen is the single most abundant element in the Universe, amounting to more than 90% of the total atoms on the observable universe. It is the lightest element and it is known to have the highest energy content by weight, 119.96 MJ kg^{-1} [5], providing almost double the amount of energy than most conventional fuels.

Even though hydrogen is undoubtedly abundant, it is not naturally found in its atomic form (H), existing only as H_2. However, hydrogen (or H_2 gas) is very rarely encountered on Earth, as it is mostly found chemically bonded in several compounds, such as water or water vapor, and most organic compounds. Luckily, hydrogen can be produced by almost all energy sources [6], given its abundancy, so there is certainly no shortage of methods for its production, which will be discussed in more detail later in this work.

1.1.1 Hydrogen and its Applications

In what concerns the industry, H_2 has three primary applications that contribute the most to the overall hydrogen economy: industrial feedstock (ammonia and methanol production), refinery applications (crude oil processing) and industrial energy. To put this into perspective, about 55% of the hydrogen produced around the world is used for ammonia synthesis, 25% in refineries and about 10% for methanol production, and the rest is allocated to all other types, including its industrial applications [5] [7].

Its first application, the utilization of H_2 as feedstock to ammonia production is maybe its main direct employment. Ammonia (NH_3) is industrially obtained by the Haber-Bosch process, through the catalytic reaction between N_2 and H_2. Methanol production is also worth mentioning and, in this process, H_2 is used as a reactant in the catalytic hydrogenation of carbon monoxide [5].

The refinery industry has high demands for hydrogen gas, for the production of lighter oil products, such as naphtha, petrol or even diesel fuels. In general, hydrogen comes as a byproduct of the catalytic reforming of naphtha, which is then recycled for the hydro treatment of oil products that have high sulfur contents. Hydrocracking also plays an important role in the refinery industry as the hydrogen used is now sourced elsewhere because the H_2 produced by the catalytic reforming of naphtha is no longer sufficient, and its source is equally carbonizing.

On the other hand, inside the industrial energy sector, hydrogen is a secondary energy source and chemical energy storage gas, used primarily as heat engine combustion fuel or in galvanic fuel cells. The latter is an extensive area of application, but briefly explained by the operation of a fuel cell — fuel cells convert chemical energy into electrical energy directly.

As for the transportation sector, hydrogen is proving itself to be the most viable energy source yet, given the extreme difficulty of decarbonizing this sector. When directly applied, hydrogen is used as an energy source, without further conversion, in both internal combustion engines and fuel cells. On the other hand, hydrogen can be indirectly employed as a mean of producing final energy sources, or even further converted into gaseous or liquid hydrogen-containing fuels. H_2 has vast mobility applications in several fields like space travel, aviation, nautical transportation, rail and vehicles (domestic cars and industrial trucks), like the case of Fuel Cell Electrical Vehicles (FCEVs) which are currently in both production and use [5].

These applications are still very environmentally harmful because the hydrogen in use is mainly sourced from steam methane reforming or from the gasification of coal, which are extremely polluting. In theory, utilizing clean hydrogen is the ideal scenario, and it is already being implemented into some of the main applications.

1.1.2 Hydrogen Production

H_2 is already mass produced worldwide, through processes from fossil fuels, biomass or water, which are better explained later, in Chapter 2. Currently, hydrogen is produced at a yearly rate of 70 Mt [8], worldwide, and is largely produced through natural gas, around 76%, followed by coal, at 23% and less than 0.1% of the hydrogen production comes from water electrolysis. H_2 is producing CO_2, between all of these production methods, at around 830 Mt_{CO2} $year^{-1}$ [6]. H_2 production rates are announced to reach an outstanding 520 Mt $year^{-1}$ by 2070, which can reduce CO2 emissions by a whopping 2.96 Gt_{H2} [6].

As for hydrogen demand, it is now circling around the 74 Mt each year (IEA, 2018) [9], and expected to increase to around 500 Mt $year^{-1}$ by 2070, following a sustainable scenario for the future, with different sectors set to increase different amounts [9]. From the ammonia and methanol industries, H_2 demand is set to increase by 1.7% and 3.8%, respectively, in 10 years. These industries produce high amounts of undesirable CO_2 (630 Mt_{CO2} $year^{-1}$) [9]. The European Union also contributes to the H_2 production, with 7.8 Mt of H_2 produced in 2010 (from a total yearly production of nearly 50 Mt, around 16%) [7] H_2 is being produced at a cost of 1.50 € kg^{-1}, via methane steam reforming, which is usually put into perspective when comparing the estimated costs of clean hydrogen, standing at 3.85 € kg^{-1}, at the maximum [7], [9]. It is clear that clean hydrogen is not yet very cost-competitive in comparison. Current estimates, from the International Energy Agency (IEA), about public hydrogen R&D expenditures worldwide are looking at a staggering 1 billion USD per year, which is still modest when compared to other energy R&D costs. From this estimate, Japan, the USA and the European Union are at the frontline, accounting for about 66% of the budget [3].

1.2 The Hydrogen Economy — Opportunities and Challenges

The hydrogen economy, at this moment, is fast-growing and flourishing worldwide. It is described as a suitable economy where hydrogen is an energy carrier capable of delivering a substantial fraction of all energy production and use, and is considered to be the main objective of H_2 as a whole [4]. The economy can be subdivided into the hydrogen production and consumption and the hydrogen market itself, covering everything from the production lines to its last application. In such an economy, hydrogen fulfills many of its applications, directly or indirectly related to energy, or even unrelated whatsoever, roughly divided into the industry itself, the transportation sector and the energy sector.

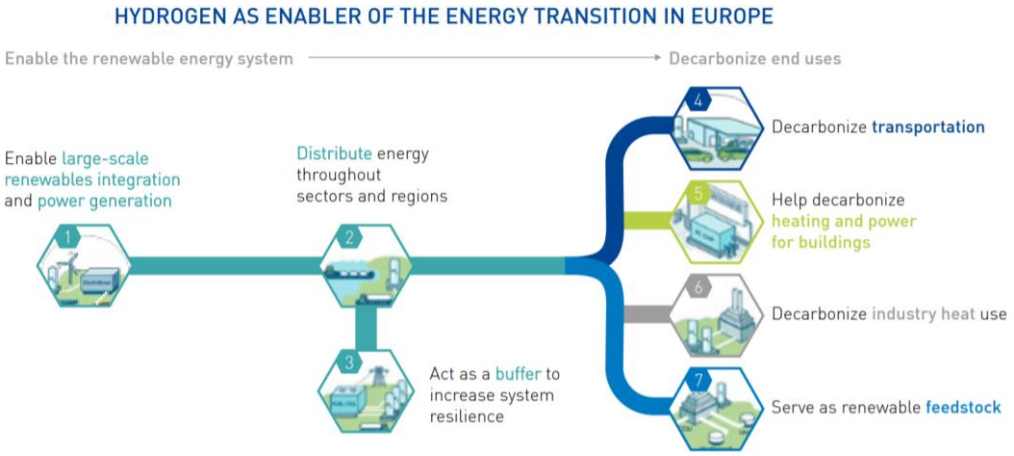

Figure 2 — Hydrogen as an enabler for the transition to a future neutral energy scenario. Retrieved from [3].

Europe, for instance, has a clear objective on the climate change mitigation, specifically on the introduction of hydrogen as a substantial fraction of the energy transactions in the future.

In the European economy, H_2 is supposed to enter the field gradually, until full decarbonization is attained, in 2050 [10]. The EU is now focusing on the improvement and development of reliable hydrogen production methods, that can help achieve such a future energetic scenario, briefly described in Figure 2, highlighted by the replacement of fossil fuels by RES, introducing a renewable energy system (in which H_2 is a key player) to then achieve carbon neutrality.

Ultimately, hydrogen is establishing itself as a competitor in both business and economic aspects, so hopefully it can reach its full potential as the ideal sustainable energy carrier of the future. Several methods of clean H_2 production are now being thoroughly studied to start the transition to a more carbon neutral society, bringing a special focus to the photocatalytic processes, which employ solar light as a source of radiation to produce hydrogen gas.

1.3 Organization of the dissertation

This Master's Thesis is organized by chapters divided into the Introduction, Context and State-of-the-art, Materials and Methods, Results and Discussion, Conclusion and Work Assessment, conveniently referenced in the last chapter.

In Chapter 1, the Introduction, there is a brief explanation of the problems to be solved, and how they can be effectively eliminated, where hydrogen is introduced as the best future energy carrier, which can decarbonize the economy to hopefully attain the worldwide objectives to its deployment.

In Chapter 2, the Context and State-of-the-art, there is an extensive presentation of the processes involved in the work, as well as the current technologies and development strategies in terms of hydrogen production. The intricate photocatalytic reaction mechanisms are also explained in detail.

Chapter 3, Materials and Methods, describes the procedures and installations used in this work, detailing all of the materials and methods employed to obtain the results. The analytical methods used to quantify the products of the reactions are also described in this Chapter.

In Chapter 4, Results and Discussion, the obtained results from all of the conducted experiments on the photocatalytic hydrogen production, and the influence of some variables, are presented and discussed.

In Chapter 5, the Conclusion, the conclusions made from the previous Chapter 4 are listed. Finally, in Chapter 6, the Work Assessment, the objectives of this dissertation are assessed and evaluated, if they were attained or not, and future prospects and suggestions are also provided.

2 Context and State of the art

2.1 Hydrogen Production Methods

Clean hydrogen as an energy system is still not a reality, but rather a safe and sustainable expectation of the integration of this vector as a considerable fraction of the energy scenario in the near future. Furthermore, the production methods currently employed to produce H_2 are still very environmentally harmful and if hydrogen is designed to reach its full potential as an energy vector in a decarbonized economy, it needs to be mass produced in a sustainable way to become cost-competitive with conventional fuels.

H_2 can be produced through several processes, commonly categorized into electrolysis, biochemical conversion and thermochemical conversion, which includes steam reforming (also known as methane steam reforming — MSR), partial oxidation and autothermal reforming with some being carbonizing, while others are carbon neutral [5].

Hydrogen is primarily produced from fossil fuels — by steam reforming of natural gas or gasification of coal, which is a thermochemical method of production that contributes to the CO_2 problem aggravation, and as of 2019, almost 95% of the total hydrogen production came from this process [7]. The thermochemical methods of H_2 production are briefly explained in Table 1.

Table 1 — Thermochemical methods of hydrogen production [5]

Thermochemical Methods of H_2 Production	
Steam reforming / Methane Steam Reforming (MSR)	Water is used as an oxidant in the endothermic reaction (introduction of heat is necessary). The raw materials used are mainly steam and natural gas, which need to be pretreated to remove sulfur contamination (it attacks the catalyst). The products are mainly H_2 and CO, with other gases in residual amounts. Addition reactions to the remaining water and CO are conducted to produce more H_2, through water gas shift reaction.
Partial Oxidation (POX)	It is an exothermic (releases heat) conversion of mainly heavy hydrocarbons ($C_{16}H_{34}$ — hexadecane, for instance), aided by oxygen (or air). It occurs at high temperatures, between 1250 and 1400 ºC, and it yields more hydrogen when shorter chained hydrocarbons are used. POX is less efficient compared to MSR, but it can convert a much wider range of raw materials.
Autothermal Reforming (ATR)	It is a combination of MSR and POX and operates utilizing a mixture of air and water vapor. The objective is to turn ATR into a thermoneutral process. The hydrogen yield is controlled by the SMR step and the overall necessary heat is supplied by the POX step.

In what concerns biochemical conversion, H_2 is mainly produced by microorganisms through substrate fermentation and further conversion, or by water splitting (biophotolysis). Several methods are available for the conversion of sugars, starches and lignocellulosic biomass into

hydrogen, using mostly sunlight as a radiation source. One limitation shared between all biochemical processes is the fact that it only exists at laboratory scales.

Electrolysis is also a part of the hydrogen production worldwide, by enabling the production of hydrogen from electricity and water. This technology is presently applied in several sectors of the industry but is now more focused on energy and climate change objectives like vehicle fueling, using hydrogen as an input for industrial processes, electricity storage and synthetic fuel manufacturing.

Ultimately, hydrogen is still produced by methods that are either still too carbonizing in general, extremely expensive, or immature and in need of further development, so their substitution is optimal [11]. Recent advances on clean hydrogen production mark photocatalysis as the key to meet future energy requirements in terms of H_2 production. Since photocatalysis is done under solar irradiation, harvesting this energy source (by absorption and conversion) seems to be the most efficient and environmentally friendly, as it has zero GHG emissions.

Photocatalytic hydrogen production has been subjected to heavy research for some time now. The possibility of using alcohols like methanol, ethanol and glycerol, which can be found in waste streams of several industries, as a way to produce H_2 brought attention to this process. The base reactions are conducted under all sorts of radiation types, but most use solar and UV light (or lamps that closely simulate the solar light wavelength range), to provide better understanding of the possibility of employing this renewable energy source in these processes.

Interestingly, glycerol has been shown to give the best results in the photocatalytic hydrogen production processes. This can be attributed to several factors, like polarity, number of α-H (alpha hydrogen) atoms and number of hydroxyl groups [12]. Although the advantages are indeed appealing, it is worth noting that, for example, against ethanol, glycerol leads to the catalyst deactivation much faster, because of the vast range of intermediates that can form when glycerol is being degraded.

To bring circular economy into this process, as residue and waste valorization is now an important focus point for any process, utilizing waste products from other industries brings a new pathway for the production of hydrogen, given the abundancy of glycerol as a waste by-product of the biodiesel production industry.

2.2 Hydrogen Production from Biodiesel By-Products

Biodiesel is a biofuel that consists mainly of long-chain esters, derived from animal or plant sources. It is currently produced by a transesterification reaction, both at small scales or industrially, using vegetable oil, animal fat and other non-edible materials as raw-materials.

This reaction has some by-products, but it mainly produces glycerol as a secondary product, given that a 100 kg of glycerol are produced alongside each ton of biodiesel produced [13].

Glycerol is, therefore, a significant by-product stream of the global biodiesel production since biodiesel reached production quantities of 129 million liters in 2019 alone [14]. This molecule has a great range of applications, in various sectors, from food and tobacco, cosmetic, paint, pharmaceutical and even paper, leather and other textile industries [12]. These are the applications where pure glycerol is employed, commercially and industrially, but crude glycerol is excluded. Instinctively, crude glycerol from biodiesel production is impure since it has great amounts of other components like methanol, oils, soap and even solid organic materials, which can make up from 25 to 35% of the total crude glycerol content.

Crude glycerol is, therefore, technically a different substance. Its impurities can severely restrict its applications, mainly when competing with its pure counterpart, making crude glycerol an almost obsolete by-product when untreated [12]. Moreover, the treatment, or purification, of crude glycerol is very expensive. So, many industries end up resorting to burning it to obtain energy, which is very counter-productive, both economically and environmentally, since its energy content value is very low.

Because glycerol is a highly functionalized molecule, and an extremely important industrial by-product, it has to be valorized in order to reduce waste whilst giving a new purpose to this otherwise very irrelevant material. Its valorization can be done through several processes like dehydration, dehydrogenation, pyrolysis and gasification, each resulting in several different compounds, the so-called value-added products [15]. These compounds can be either liquids or gases, like dihydroxyacetone, glyceraldehyde, acrolein, hydrogen, among others [13].

One valorization pathway is the aforementioned photocatalytic hydrogen production, which might be the key to meet a greener future, as it uses radiation as an energy source. Thus, if the radiation type is chosen to be solar light, which seems to be efficient in water splitting and redox reactions present in this type of process, this can assure the sustainability of the whole process. This process is usually conducted at mild temperature and pressure conditions, usually in the 25—70 ºC range and at the atmospheric pressure, using aqueous solutions of water and alcohols. These alcohols, especially at low concentrations, can be very beneficial to the process because they change the limiting step of the overall reaction from water splitting to alcohol conversion, which significantly increases the overall rate of hydrogen production.

Surprisingly, glycerol showed very good results in the photocatalytic production of hydrogen, when compared to other alcohols such as ethanol and methanol [12].

2.2.1 Photocatalysis

Catalysis, the base process of photocatalysis, can be briefly described as a process in which chemical reactions are conducted in the presence of catalysts, which is not consumed during the process. This lowers the overall activation energy, E_{act}, which consequently increases the rate of the reaction. This process is then divided into different types of catalysis, namely, homogenous, heterogeneous and enzymatic catalysis, described as follows [16]:

Homogeneous Catalysis: The bulk (reactants) and the catalyst are both in the same phase; **Heterogeneous Catalysis:** The bulk and the catalyst are in different phases, and the reactions occur at the interface created between the two phases. The reaction itself occurs at the active sites of the catalyst; **Enzymatic Catalysis:** The catalyst is an enzyme, a macromolecule capable of metabolizing substrates at their active sites, described as a mixed type of catalysis.

Heterogeneous catalysis is the most industrially employed to mass produce several chemicals, providing almost 90% of all industrial chemical compounds. The use of solid materials to catalyze reactions can improve not only their production rates, but it can also reduce production times and improve purity and selectivity. Heterogeneous photocatalysis (denoted by photocatalysis hereafter) is a clear variant of a heterogeneous catalysis process, since it employs solid photocatalysts in aqueous solutions. XX

Photocatalysis is described, in practical terms, as the conversion of photonic energy into chemical energy, through absorption of light by a photocatalyst (usually a semiconductor), divided into five steps, in Figure 3.

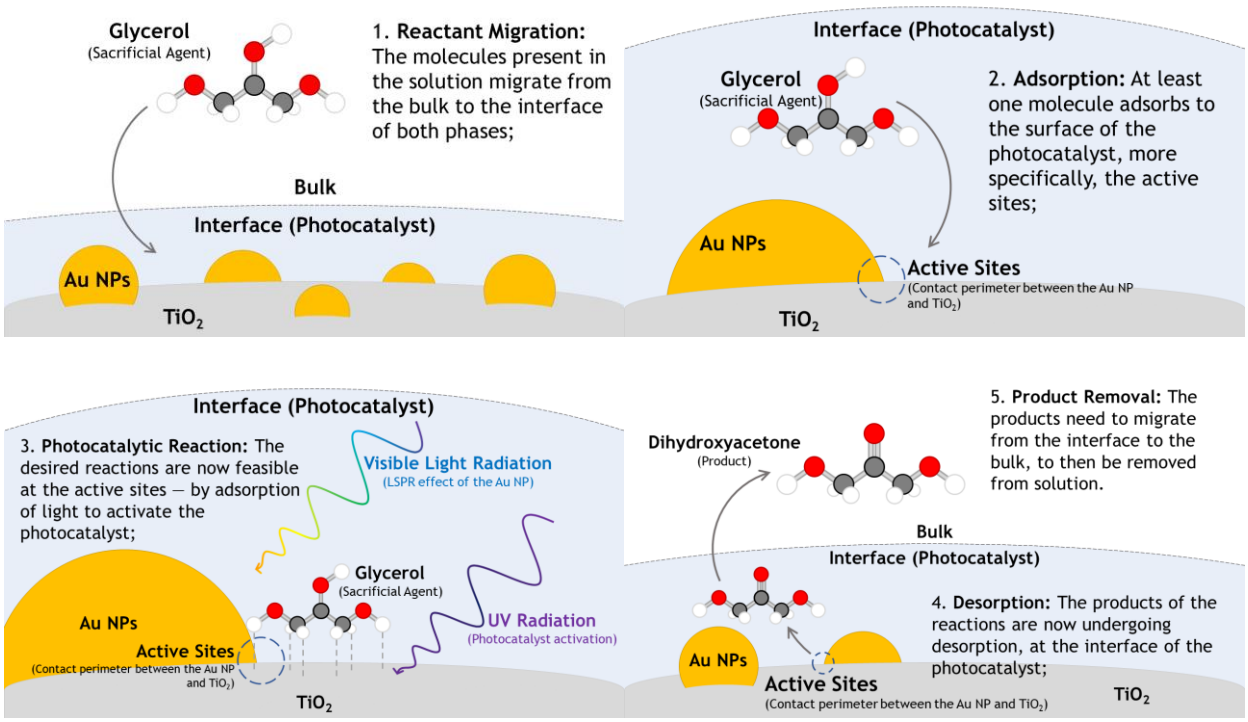

Figure 3 — Scheme of the 5 steps of the photocatalytic reaction in AuNPs (gold nanoparticles).

Because photocatalysis is a surface phenomenon, various factors influence the efficiency and performance of the process, including crystal size, morphology, crystalline phase, specific surface area, pore size and pore volume, among others. The choice of the photocatalyst is a crucial step that drastically influences the overall efficiency of the process.

2.2.1.1 Semiconductors as Photocatalysts

Photocatalysts used in this process are usually semiconductors because of their capability of harvesting solar power as a radiation source.

Semiconductors have interesting electronic properties, which make them a unique material because unlike metals, semiconductors have a band gap — an electronic vacancy that separates the empty Conduction Band (CB) and the filled Valence Band (VB), where no electronic states can exist (Figure 4), explained by the band gap theory, based on the mechanical-statistical extension of the atomic model proposed by Bohr.

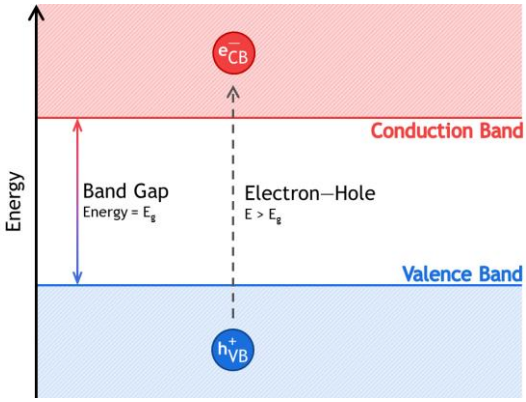

Figure 4 — Schematic representation of the charge carrier separation in a semiconductor, of band gap energy E_g.

Because no electronic levels are available, semiconductors only become electric conductors when irradiated with sufficient energy, greater than the band gap energy, E_g — the necessary energy to excite a valence electron from the VB to the CB, or the difference between the CB (or its lowest energy, E_C) and the VB (or its highest energy, E_V), measured in electron-volt, eV. Different types of semiconductors have different band gap energies, as seen in Figure 4.

Upon irradiation, the electrons in the VB are excited to the CB, leaving holes behind, forming an electron-hole pair, e^-/h^+. These two charge carriers, separated only by the band gap, are now free to move within their electronic state, being capable of interacting with the bulk to trigger of redox reactions. The electron-hole pair has a lifetime of some nanoseconds, so their recombination rate is high. If the pair recombines, the reactions cannot happen because no charge carriers are available to conduct reactions, which deactivate the photocatalyst, so recombination must be avoided or disabled.

The most common semiconductors are crystalline solids, involving elements located near the metalloid region of the periodic table, like silicon, germanium or gallium, although some others are also commonly used, like titanium. TiO_2 has been, for some time now, the semiconductor of choice to conduct photocatalytic processes, as researchers found it is capable of absorbing UV light.

2.2.1.1.1 Titanium Dioxide (TiO_2)

Titanium dioxide, or titania, is a natural titanium oxide, normally a white powder, found in food coloring, sunscreen and paints. This material can be found in several distinct crystalline structures, but there are three main structures, anatase, rutile and brookite, whose unit cell configurations are depicted in Figure 5 [17]. Because the differences between them have to do with the crystalline structure and chemical bonding of the material (unit cell configuration), its properties are altered from one to the other, primarily in the band gap energy, density and in the electronic band structure.

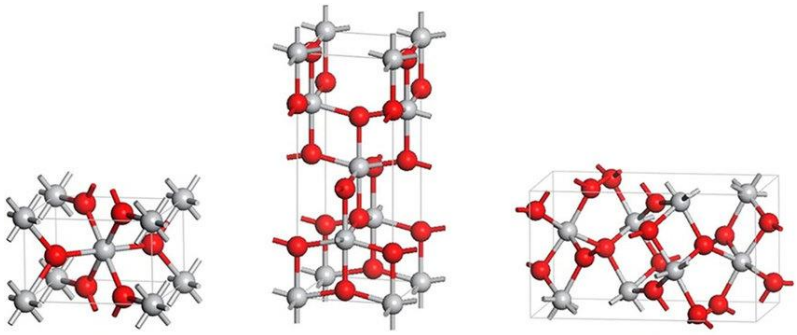

Figure 5 — Unit cell configuration for anatase, rutile and brookite, respectively. Adapted from [17]

TiO_2 has been widely employed as a photocatalyst, due to its excellent chemical and physical stability, extensive availability, non-corrosive and non-toxic and, although the phase of this material may not always be the same, its advantages stay constant for all of them. Nevertheless, titania is still suffering from some disadvantages, which can restrict its practical applications, especially in photocatalysis. Titania has a high recombination rate of the generated electron-hole pairs, limiting the efficiency of the photocatalytic reaction, so lower rates of chemical transformations are observed. It is also well known that TiO_2 has a band gap energy of around 3.2 eV [18], so UV radiation is necessary to activate the semiconductor. Using sunlight as a radiation source proves to be inefficient because TiO_2 only absorbs about 5% of the solar spectrum. These to phenomena are indeed the two main problems of TiO_2.

To counter this problem, titania must be improved as a photocatalyst, to be efficiently employed in these reactions. Recombination rates of electron-hole pairs and photoactivation can be manipulated by modifying the semiconductor itself. Many efforts are being directed into the optimization of such modifications, and over the last years, much progress has been achieved. Many different types of modifications have been proven to enhance the performance

of this semiconductor, such as metal and non-metal doping, dye sensitization, surface modification, fabrication of composites with other materials and immobilization and stabilization on support structures [19].

Modifying a semiconductor changes the initial properties, inhibiting or enhancing them, to finely tune the desired final properties of the resulting material, which can be better recombination inhibition, better light absorption, among others. Doping is probably the most used to change the properties of these semiconductors due to the extensive research put into it.

2.2.1.2 Doping Semiconductors

Doping a semiconductor is a rather simple way to shift, narrow or broaden its band gap, altering its intrinsic properties by depositing foreign particles at its surface. In a semiconductor alone, the only charge carrier transfer processes are the electron-hole separation and recombination, controlled by the high recombination rate. When a semiconductor is doped, its band gap shifts, which can be tuned to optimize the absorption of radiation in the visible light spectrum to use solar radiation as a source, which is one of the main pillars of photocatalytic processes. Doping also alters the reaction mechanisms by providing new and improved active sites at the interface of the photocatalyst.

Gold was long thought to have no catalytic interest because of its chemical inertness, at a macroscale. Only when dispersed at the nanoparticle scale, this metal proves to be very chemically active and it can highly improve the efficiency of the photocatalyst, so many researchers directed their efforts into developing preparation methods to ensure the production of active and stable photocatalysts [20].

Depositing gold at a small scale was found to be crucial to hinder the electron-hole pair recombination rates, given that Au acts as an electron sink [19]. Gold nanoparticles also contribute to the absorption of solar light since the nanoparticles are capable of shifting the wide band gap of the doped semiconductors into the visible light range. Nevertheless, this phenomenon is largely affected by particle size and shape [17], which are strongly influenced by the method of preparation used to produce the photocatalyst.

2.2.1.3 Au/TiO_2 Photocatalyst Preparation Methods

Gold-doped photocatalysts can be prepared by many different ways, but they are typically prepared by methods like impregnation (wet and/or dry), hydrothermal and solvothermal techniques, co-deposition, photo-deposition, chemical vapor deposition, sol-gel methods, and deposition-precipitation. The last is the most typical method used to produce photocatalysts due to the simplicity of the procedure in comparison, resulting in good and efficient photocatalysts.

2.2.1.3.1 Deposition-Precipitation (DP)

Deposition-precipitation (DP) methods are among the most utilized when producing doped metal oxide catalysts, especially gold-doped titania [20]. This preparation method is quite simple conducted at low temperatures and fixed pH values. This method, developed by Haruta [20], is composed of two main processes. The first is the precipitation step, which is the creation of a solid from a liquid solution using a precursor (usually gold chloride or chloroauric acid), and the second is its deposition onto the surface, which is the interaction between the precipitate particles and the surface of the support. Both the precipitation and the deposition are steered to take place exclusively at the surface of the support. This method of preparation leads to very good nanoparticle dispersion, with very low particle sizes (typically 3—4 nm). Although beneficial, as it is widely understood that low diameters particle at the surface of the support leads to high catalyst efficiency, this process requires careful control of several variables to ensure the efficiency of the process.

Deposition-Precipitation method has some disadvantages that can affect the efficiency and performance of the catalysts. It seems to be ineffective when the support used has a point of zero charge (pzc) below 5, so that excludes silica, for example [20].

Because the precursor (gold chloride or chloroauric acid) is hydrolyzed into gold and chloride ions, the latter stay in solution after precipitation. They are known to affect the efficiency of the photocatalyst so washing steps are necessary to remove the Cl^- ions from the obtained samples, because even small concentrations of Cl^- in solution can affect the efficiency of the photocatalyst by causing particle agglomeration, diminishing the total surface active sites.

This process is highly sensitive to the operation conditions, especially (but not limited to) pH values. Some researchers found optimal pH values in the basic range, from 7—10, with an optimum gold loading at a pH value of 8 [21]. This results in the almost complete removal of Cl^- from the gold complexes by hydrolysis. The pH is always carefully controlled during photocatalyst preparation by adding a base to the solution, normally sodium hydroxide injections or urea hydrolysis. At a pH of 8, the dominating species in solution are both $[AuCl_2(OH)_2]^-$ and $[AuCl(OH)_3]^-$, gold complexes that are deposited at the surface via a grafting reaction with the existing surface hydroxyl groups, as stated in Equation (1). After the DP procedure is complete, the surface gold complexes are reduced from Au^{3+} to Au^0, by existing Ti^{4+} in the semiconductor.

$$TiOH + [AuCl(OH)_3]^- \rightarrow Ti{-}[O{-}Au(OH)_3]^- + H^+ + Cl^- \quad (1)$$

2.2.1.4 Photocatalytic Reaction Mechanisms of Doped Semiconductors as a Photocatalyst

As stated before, a semiconductor only has electron-hole pair mediated reactions, only affected by the recombination rate of the charge carriers of the semiconductor itself, which is high for

TiO_2. However, when a doped semiconductor is employed, the mechanisms are inherently altered, changing the interactions between the molecules and the catalyst.

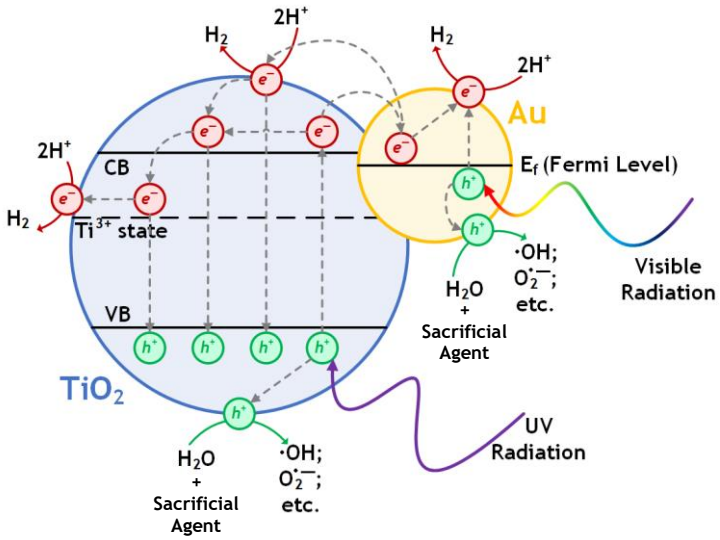

Figure 6 — Charge carrier transitions and photocatalytic reactions, using a gold catalyst (Au/TiO_2) and an aqueous sacrificial agent solution.

Figure 6 depicts several possible steps of a photocatalytic reaction using a doped semiconductor in an aqueous solution of a sacrificial agent. First, the catalyst is irradiated, using a source in the visible or UV range, which promotes the photoexcitation of the electrons present in the valence band. This excites the electrons (e^-_{CB}) into the conduction Band, which was previously empty, leaving behind its counterpart, the hole (h^+_{VB}), forming an electron—hole pair, which are now separated by the bandgap of the semiconductor, shown in Equation (2).

$$TiO_2 + hv \rightarrow e^-_{CB} + h^+_{VB} \quad (2)$$

Because both of these species are in different bands, and free to move within them, they can either interact with other present species or recombine, as described by Equation (3).

$$e^-_{CB} + h^+_{VB} \rightarrow \text{heat} \quad (3)$$

If an electron spends enough time in the CB of the semiconductor (avoiding recombination), it can travel to its surface by self-reduction of Ti^{4+} to Ti^{3+}, creating a lower energy state, like an impurity or defect, and can promote redox reactions. This exited electron can trigger the reduction of H^+ ions into H_2 molecules.

2.2.1.4.1 Glycerol as a Sacrificial Agent

Photocatalytic reactions use alcohols as sacrificial agents in the reactional media to undergo redox reactions at the surface of the photocatalyst, as the alcohols will now be preferentially oxidized (photo-reforming), though water molecules will also be oxidized through water splitting [22] [23]. This method is commonly referred to as sacrificial H_2 production, which is

far more effective when compared with water splitting without sacrificial agents, providing a convenient method to generate H_2, seen in the stoichiometry in Equation (4).

$$C_3H_8O_3 + H_2O \xrightarrow{hv,\ Au/TiO_2} CO_2 + 7H_2 \quad (4)$$

Glycerol acts as a hole scavenger when adsorbed at the surface of the photocatalyst employing glycerol as the sacrificial agent, is in Equation (4). Several properties of the commonly used molecules often dictate how well a molecule can act as a sacrificial agent, and therefore they can, to some extent, dictate the overall hydrogen production. Some researchers found influential properties to be the oxidation potential, which is very low for glycerol when compared to other alcohols (0.004 V), making them efficient hole scavengers. Chen et al. (2015) found linear relationships for all of the referred properties, proving glycerol as the best sacrificial agent, as it performed the best for every Au/TiO_2 photocatalyst system [22].

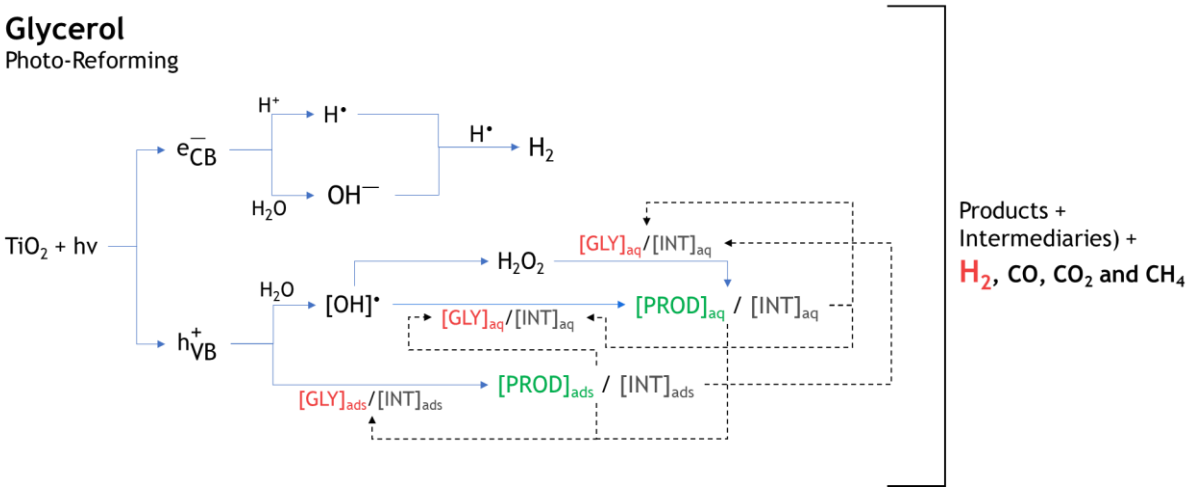

Figure 7 — Reaction pathways for the conversion of glycerol into hydrogen. ([GLY], [INT] and [PROD] stand for glycerol, intermediary, product; subscripts "aq" and "ads" stand for aqueous and adsorbed, respectively. Adapted from [12].

There are two types of mechanisms for the charge carriers: the photo-generated hole can directly react with adsorbed glycerol (hole-mediated mechanism) to then form adsorbed products and intermediates (like glyceraldehyde, dihydroxyacetone, acrolein, pyruvic acid, among others), but they can also interact with water molecules, to trigger water splitting, generating hydroxyl radicals (radical-mediated mechanism) which then enable reactions between them and aqueous glycerol and intermediates. These hydroxyl radicals can also auto-react, forming hydrogen peroxide (H_2O_2), a highly reactive species that can also interact and produce intermediates, or can be further oxidized to generate products [12].

The glycerol molecules are then degraded by this mechanism, forming either products or intermediaries, as proposed in the reaction network in Annex A.

2.3 Objectives of the Dissertation

The main objectives of this dissertation are the evaluation of the hydrogen production through photocatalysis using an aqueous glycerol solution (acting as the sacrificial agent), using Au/TiO_2 as a photocatalyst. Glycerol is a significant by-product of the biodiesel industry, which is not commercially important, so aiming for its valorization by means of photocatalysis is another objective of the process.

The second main objective was to find the best conditions to conduct the photocatalytic process. To achieve this, different parameters and variables were changed, mainly the calcination pretreatment of the photocatalyst, Au/TiO_2 particle size, gold loading, initial pH and temperature. Finally, with the best operation conditions found, a long-term run would be carried out to study the stability of the process in terms of hydrogen production.

Table 2 — Photocatalytic hydrogen production through sacrificial agent degradation.

Catalyst System	Preparation Method	Cocatalyst Dosage	Sacrificial Agent	Sacrificial Agent Concentration	Reaction Conditions	H_2 Production		Ref.
		%(wt)		%(v/v)				
Cu/TiO_2	WIMP	1.30	Glycerol	10.00		2061	μmol g^{-1} h^{-1}	[24]
Cu/TiO_2	SG	10.00	Glycerol	10.00	500 W halogen lamp (400 — 650 nm)	2114.2	μmol h^{-1}	[24]
Cu/TiO_2	Reduction of cupric ions	9.22	Glycerol	10.00	125 W high pressure mercury vapor lamp (305, 313 and 366 nm)	1 — 7	μmol min^{-1}	[24]
Co/TiO_2	IMP	1.00	Glycerol	5.00	Solar light and UV radiation (400W Hg vapor lamp (184 — 600 nm))	11021	μmol g^{-1} h^{-1}	[24]
Au/TiO_2	DPU	0.25	Methanol	50.00	Green, Blue and Purple lamps 913W (UV range: 250 — 400 nm; Visible range: 400 — 700 nm)	1032	μmol g^{-1} h^{-1}	[25]
Au/TiO_2	DPU	0.50	Methanol	50.00	Green, Blue and Purple lamps 913W (UV range: 250 — 400 nm; Visible range: 400 — 700 nm)	2336	μmol g^{-1} h^{-1}	[25]
Au/TiO_2	DPU	1.50	Glycerol	10.00	Green, Blue and Purple lamps 913W (UV range: 250 — 400 nm; Visible range: 400 — 700 nm)	1536	μmol g^{-1} h^{-1}	[25]
Au/TiO_2	DPU	0.50	Methanol		UV PC Hg lamp, (254 nm, I = 2.2 mW cm^{-2})	1492	μmol g^{-1} h^{-1}	[26]
Au/TiO_2	HT	1.50	Glycerol	10.00	100 W lamp (365 nm, I = 6.5 mW cm^{-2})	27900	μmol g^{-1} h^{-1}	[22]
Au/TiO_2		1.00	Methanol	0.10	400 W Xe arc lamp	8.8	mL h^{-1}	[27]
Au/TiO_2		1.00	Methanol	50.00	24 W Xe lamp, UV; Reactor Volume = 10 mL	8400	μmol g^{-1} h^{-1}	[27]
Au/TiO_2		2.00	Glycerol	1.00	150 W Metal halide lamp, Visible; Reactor Volume = 100 mL	120	μmol min^{-1}	[27]
Au/TiO_2		2.00	Methanol	0.01	Sunlight (0,3—0,4 mW cm^{-2}); Reactor Volume = 60 mL	400	μmol g^{-1} h^{-1}	[28]

Catalyst System	Preparation Method	Cocatalyst Dosage	Sacrificial Agent	Sacrificial Agent Concentration	Reaction Conditions	H_2 Production		Ref.
		%(wt)		%(v/v)				
Au/TiO_2		1.00	Methanol	0.05	450 W Hg lamp; Reactor Volume = 340 mL	30667	μmol g^{-1} h^{-1}	[28]
Au/TiO_2		4.00	Ethanol	70.00	90 W lamp, UV; Reactor Volume = 100 mL	1.0	μmol m^{-2} min^{-1}	[28]
Au/TiO_2			Methanol		300 W Xe lamp	3550	μmol g^{-1} h^{-1}	[28]
Au/TiO_2			Ethanol		300 W Xe lamp	4900	μmol g^{-1} h^{-1}	[28]
Au/TiO_2					300 W Xe lamp; Quartz Reactor	11595.6	μmol g^{-1} h^{-1}	[29]
Au/TiO_2					100 W SB-100P/F lamp (365 nm); Pyrex Reactor	30300	μmol g^{-1} h^{-1}	[29]
Au/TiO_2					Visible light (420 nm)	924	μmol g^{-1} h^{-1}	[29]
Au/TiO_2					150 W Ceramic metal halide lamp (solar light simulation); Quartz Reactor	500	μmol g^{-1} h^{-1}	[29]
Au/TiO_2					UV-light He-Cd laser (325 nm); Quartz Reactor	125	μL cm^{-2} h^{-1}	[29]
Au/TiO_2			Methanol		300 W UV and Visible light (AIM filter); Borosil Reactor	307 (UV) 66 (Vis)	μmol g^{-1} h^{-1}	[29]
Au/TiO_2		2.00	Ethanol		100 W F lamp (365 nm)	32400	μmol g^{-1} h^{-1}	[29]
Au/TiO_2		1.50		10.00	Spectroline SB-100P/F lamp (I = 6,5 mW cm^{-2}), UV	27900	μmol g^{-1} h^{-1}	[29]
Au/TiO_2		0.80			15W (4) Phillips HB175 lamps	1542.9	μmol g^{-1} h^{-1}	[29]
Au/TiO_2		2.00	Glycerol	10.00	UV leds 100 W 365 nm	30300	μmol g^{-1} h^{-1}	[29]

3 Materials and Methods

3.1 Catalysts

3.1.1 TiO_2

In this work, the support used for the preparation of the photocatalysts was a commercial P25 Aeroxide TiO_2 powder (99.95%), from Acros Organics; its properties are listed in Table 3.

Table 3 — Properties of the Aeroxide TiO_2. [18]

Property	Units	Value
Surface Area, S_{BET}	$m^2\ g^{-1}$	55
Anatase:Rutile		86:14
Band Gap (Anatase), E_g	eV	3.20

3.1.2 Au and Au/TiO_2

To dope the support with gold nanoparticles, a gold precursor must be present in solution, to be precipitated exclusively onto the surface of the support. In the conducted experiments, the gold precursor used was hydrogen tetrachloroaurate(III) trihydrate, $HAuCl_4 \cdot 3H_2O$, also known as chloroauric acid, supplied by Alfa Aesar (99.99%). This is a yellowish orange crystalline powder, hygroscopic and light sensitive and the minimum Au content in $HAuCl_4 \cdot 3H_2O$ is 49.0%.

3.1.3 Other Relevant Materials

Glycerol ($C_3H_8O_3$), or liquid glycerin (from *José Manuel Gomes dos Santos, Lda.*), was used as pure glycerol (99.95%); sodium hydroxide (NaOH) solution was prepared using chemically pure sodium hydroxide pellets (from EKA Akzo Nobel Company).

3.2 Catalyst Preparation

3.2.1 Procedure — Deposition-Precipitation Method with NaOH

The photocatalysts were prepared by the deposition—precipitation method, previously described by Haruta (2004) [21], and hereby briefly summarized and represented schematically in Figure 8. Approximately 1.80 g of TiO_2 was pretreated by drying at 110 ºC for 24 hours, to eliminate any moisture and other contaminants that may be present. The TiO_2 powder was then suspended in an aqueous solution of distilled water (56 mL) and vigorously stirred (by a magnetic stirrer at 200 rpm). To dope the support, a solution of the gold precursor of a fixed concentration of 4.2×10^{-3} M was added dropwise to the solution containing the support, to initiate precipitation, using a covered separatory funnel to ensure darkness. This solution was

prepared using appropriate weighed amounts of $HAuCl_4 \cdot 3H_2O$, depending on the total desired gold loading on the final photocatalyst. For instance, a 2 $\%wt_{Au}$ final loading requires the use of 0.07344 g in 44 mL of distilled water, to then make a solution of 4.2 x 10^{-3} M.

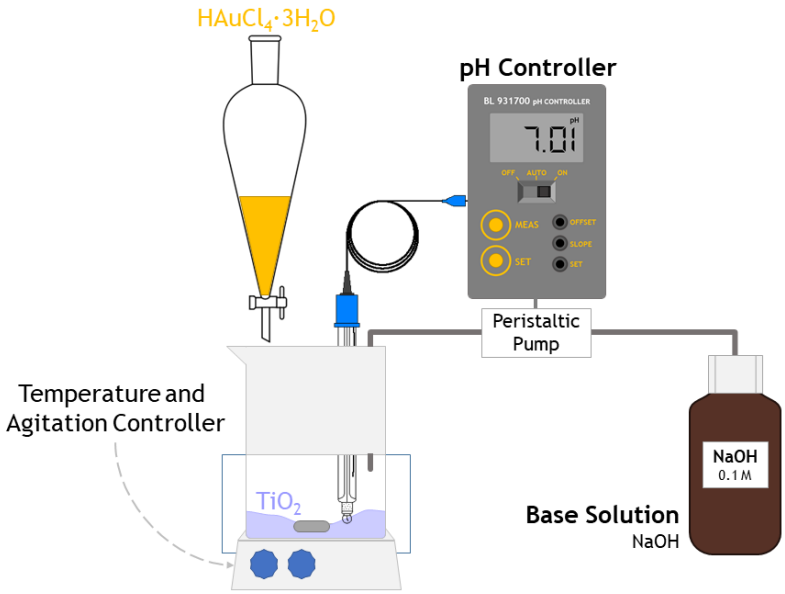

Figure 8 — Installation set-up for the photocatalyst preparation.

The pH of the solution was controlled and adjusted around a setpoint of 8.00 (±0.10), an optimal pH value found in the literature [13]. A controller from Hanna Instruments was employed by connecting it to both a pH electrode, immersed in the solution, and a peristaltic pump. The controller receives the input from the pH electrode and acts accordingly, by adding, if necessary, drops of the base solution.

The formed precipitate was aged under stirring overnight and covered to ensure darkness. This solution was then slightly uncovered to start water evaporation, maintaining the darkness of the environment as best as possible. After the evaporation step, the solid precipitate was filtered under vacuum and washed several times using 500 mL of distilled water at a temperature of around 60 ºC. The remaining solids were dried overnight at 60 ºC and then cooled to room temperature in a desiccator. The precipitate was finally milled, using an agate mortar and pestle (120 mm), and separated into two categories of particle size, 100—200 µm and < 100 µm, using a woven wire mesh sieve. The particles were stored and conveniently labeled, by their loading and size (i.e. a 2$\%wt_{Au}$ sample of size distribution between 100—200 µm, for instance, was labelled as 2%Au/TiO_2, dp = 100—200 µm).

3.2.2 Experimental Installation and Procedure

The installation used to conduct the experiments to study the photocatalytic hydrogen production from glycerol is depicted in Figure 9. The set-up is mainly constituted by the photo-reactor, a heating bath and a gas chromatograph. The central photo-reactor is a closed system

composed of a main reactor glass vessel with 1 L-capacity, in which the aqueous solution of glycerol and the photocatalyst is placed alongside a stir bar, controlled by an external magnetic stirrer plate.

The radiation source is a 150 W Hg medium pressure lamp (maximum intensity of 500 W m^{-2}), from Heraeus, with its emission spectra reported in Annex C, which is placed inside a quartz tube on top of the reactor, that emits a polychromatic light between the wavelength values of 200 and 600 nm. This lamp can reach very high temperatures, which increases the temperature of the reactional fluid, so temperature control is imperative. Therefore, the temperature is controlled by an external thermostatic bath, using an optically unreactive material such as cooling water (to ensure that all radiation can reach the reaction media), circulating inside the jacket (quartz tube) around the lamp (Figure 9). There is also an inlet stream of N_2 gas, controlled by a mass flow rate controller (from Bronkhoorst, 0—150 mL_N min^{-1}). Nitrogen serves as a purge to eliminate possible existing gases before the photocatalytic reaction is conducted, mainly atmospheric O_2. During the reaction, 25 mL_N min^{-1} of nitrogen is used as sweep gas. The outlet stream is a gaseous mixture of the fed N_2, water in gas phase and the produced H_2, with trace amounts of other possible reaction products. To remove all of the H_2O, the outlet stream is led through a Peltier condenser, which operates at temperatures close to 0 ºC. To ensure complete absence of any water, a secondary coalescence filter is placed next to the previous one. The final stream, a mixture of mainly H_2 and N_2, is now ready to be analyzed by the Gas Chromatograph, using the thermal conductivity detector (TCD).

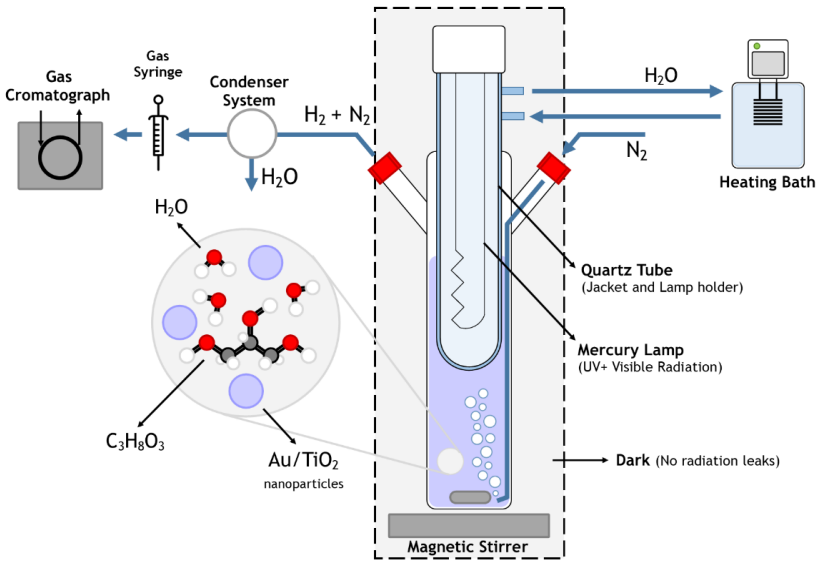

Figure 9 — Installation set-up for the photocatalytic reaction experiments.

First, a glycerol solution, of various concentrations (in volume), is prepared beforehand, and its pH levels are measured and adjusted accordingly, using a solution of NaOH (0.1 M) and a pH electrode (from Hanna Instruments). A volume of 300 mL of the solution is then placed inside the photoreactor, alongside the catalyst, at a concentration of 0.75 g L^{-1}.

Before any experiment, the photoreactor is purged of any remaining O_2 (alongside other gases that might be present inside it), with the aforementioned inlet of N_2 gas. Here, for a total of 45 minutes, N_2 is bubbled at the bottom of the reactor in two different stages of distinct flowrate. For the first 30 minutes, the flow rate of N_2 is 150 $mL_N\ min^{-1}$ to purge the system and, for 15 minutes before switching on the lamp and during the reaction, the flow rate is decreased to 25 $mL_N\ min^{-1}$. The first stage employs a much higher gas flowrate, to ensure rapid removal of the dissolved oxygen in the solution, as well as the oxygen present in the gas atmosphere inside the reactor. For the remaining time and because the purge is complete in the first step, a lower gas flowrate is employed, at the same temperature and pressure conditions. In these final 15 minutes, in each 5-minute mark, an injection in the GC must be done to obtain reference peaks of N_2, for later comparison.

The solution is now purged and ready to be irradiated, after samples of the outlet stream show the expected N_2 peaks and no existence of O_2. When the mercury lamp is turned on, the reaction media is now undergoing photocatalytic reactions. During the reaction, in pre-determined constant intervals (generally 5 minutes), an aliquot of the outlet stream is recovered, in the same fashion as the ones recovered during the purge, to then inject into the GC for sample analysis. This is conducted using an appropriate gas injection syringe (from Hamilton), of volume 100 µL, to inject the samples into the TCD detector of the gas chromatograph, to obtain and evaluate the peaks of both the products and the purge gas.

3.2.3 Analytical Methods

The amount of hydrogen produced during each experiment was determined by gas chromatography. A gas chromatograph from Agilent (model 7820A), equipped with a thermal conductivity detector (TCD), was used. The separation of H_2 occurred in a Carboxen 1010 PLOT (30 m x 320 µm x 15 µm) column using argon as carrier gas, with a flow rate of 5 $mL_N\ min^{-1}$. The temperature of the injector, oven and detector was 250, 40 and 250 ºC, respectively. A volume of 0.1 mL of sample was injected, using a split ratio of 1:5.

The pHpzc, or point of zero charge, was evaluated for a photocatalyst, 3%Au/TiO_2, by preparing two different solutions, both with a volume of 100 mL, of 5 different pH values (4, 5, 6, 7 and 8), and adding 50 mg of the catalyst to one of them, leaving one without catalyst. They were then put into an agitator, at 84 rpm, to be thoroughly mixed, at a constant rate, for 24 hours. The final pH values were then measured, to compare them with the initial pH values.

The turbidity is an optical property of solutions, that measures the extent to which radiation can pass through it, or its cloudiness. The turbidity of the initial solutions was measured using a turbidimeter from Hanna Instruments (model HI88703). The solutions of the two different particle diameters (<100 and 100—200 µm) were prepared with a 5% glycerol content (in volume).

4 Results and discussion

The reaction mechanism of the hydrogen production by photocatalysis is quite complex, being influenced by many variables, like the nature and dosage of the photocatalyst, solution pH, temperature, glycerol concentration, reactor geometry, particle size, among others. In this work, the influence of some of these variables on hydrogen production was assessed. The studied variables were, in order, material calcination temperature, particle size, gold loading, initial pH, temperature and glycerol concentration. These were all studied by following an optimization route, fixing the best result for each studied variable. Finally, an additional run of a longer reaction time (26 h) was conducted with the best conditions found.

The rate of H_2 production during the reaction is expressed in μmol g_{cat}^{-1} h^{-1}, which represents the hydrogen outlet molar flowrate at each instant, normalized by the photocatalyst mass. The total amount of H_2 produced, expressed in μmol g_{cat}^{-1}, was always calculated for the total reaction time, 3 hours, by integration of the rate of production. In the last photocatalytic experiment, the longer duration run, both CO and CO_2 were also equally quantified throughout the reaction.

4.1 Blank Tests

The photocatalytic process can be conducted only with a semiconductor, un-doped or altered. To see if the modifications done to the semiconductor are indeed beneficial, a blank test was conducted using only TiO_2 (with a particle size of 100—200 μm) as a catalyst and glycerol as sacrificial agent (a solution of 5 vol. % was employed).

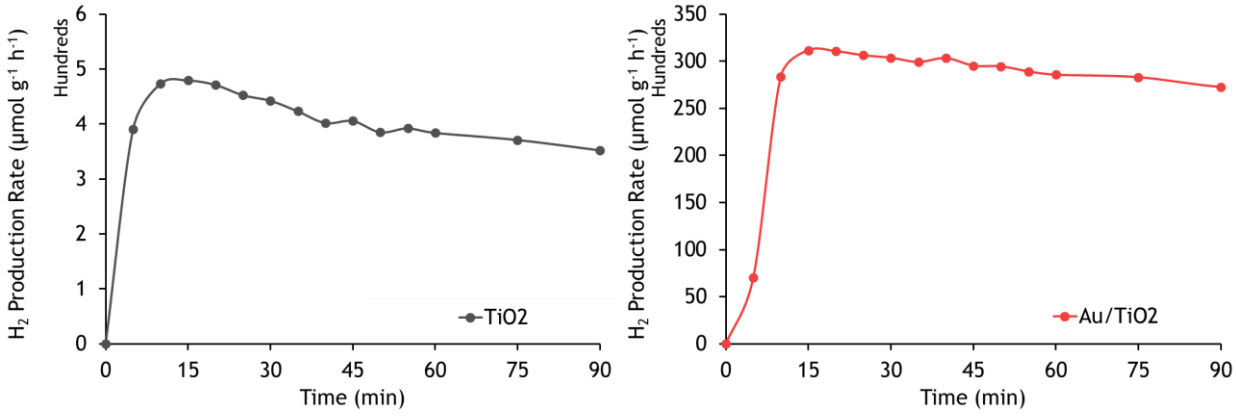

Figure 10 — H_2 production rate for TiO_2 (a) and H_2 production rate for 3%Au/TiO_2 (b) during 90 min of reaction. Conditions: T = 50 ºC; d_p = 100—200 μm; $[glycerol]_0$ = 5%(vol); V_{sol} = 300 mL; I = 500 W m^{-2}; [cat] = 0.75 g L^{-1}; Au loading = 2%; pH = 6.38.

The H_2 production observed in the blank test was very low when in comparison with the H_2 production obtained by using a gold-doped catalyst (Au/TiO_2) – please notice scales in each

figure, Figure 10 a and Figure 10 b. Gold is known to act as an electron sink, trapping charge carriers at the surface of the photocatalyst, hindering the recombination rates of the electron-hole pairs, which are then capable of reacting with the solution. For the semiconductor itself, recombination happens spontaneously at a higher rate than for the gold-doped semiconductor, which affects the hydrogen production severely, as the charge carriers are unable to spend the necessary time in their excited state, disabling the photocatalytic reactions. Figure 10 shows the results for the photocatalytic hydrogen production for the blank test against a test using a gold-doped catalyst, in which the results show a drastic increase in the H_2 production, which was to be expected.

The ineffective production of hydrogen by only TiO_2 could also be a result of the radiation in use (the lamp emission range is in Annex C), which emits light mainly in the visible light range, and TiO_2 only absorbs 5% at maximum, as it mainly absorbs UV radiation.

Another blank test was carried out in the presence of a doped catalyst (3%Au/TiO_2), but without a sacrificial agent, using just water as a reactant to see if water could be subject to photocatalytic reactions. Indeed, this blank test proves this is true, as it can be inferred by the hydrogen evolution depicted for the blank test without utilizing the sacrificial agent (Figure 11 a)). However, using a sacrificial agent in the initial solution is extremely beneficial to the hydrogen production (Figure 11 b)), which increases by a factor of ca. 108

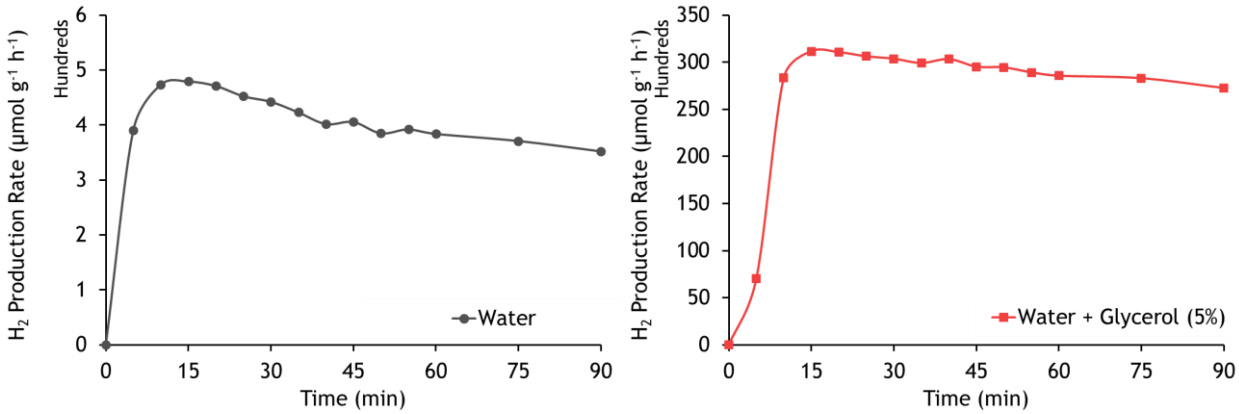

Figure 11 — H_2 production rate for 3%Au/TiO_2 with water (a) and for 3%Au/TiO_2 with water + glycerol (5%) (b) during 90 min of reaction. Conditions: T = 50 ºC; d_p = 100—200 µm; $[glycerol]_0$ = 5%(vol); V_{sol} = 300 mL; I = 500 W m^{-2}; [cat] = 0.75 g L^{-1}; Au loading = 3%; pH = 6.38.

4.2 Reproducibility

To ensure the reproducibility of the experiments, one of the experiments was doubled, in the exact same conditions, but for two different catalyst samples, of different preparations (S1 and S2). Figure 18 shows the reproducibility of the results, with the relative error, in percentage, using the sample with the lowest production values as the reference.

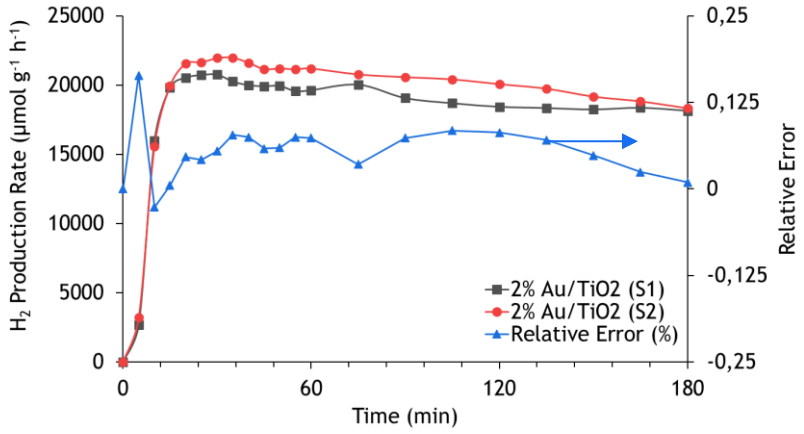

Figure 12 — H_2 production rate for two different samples in the same conditions, with relative error (with S1 as reference). Conditions: T = 50 ºC; d_p = < 100 µm; pH = 6.39; [glycerol]$_0$ = 5%(vol); V_{sol} = 300 mL; I = 500 W m^{-2}; [cat] = 0.75 g L^{-1}; Au loading = 2%.

As seen in Figure 18, the relative error between the samples (S1 reference and S2 as the replicate) is, in average, 5.3 %, which is minimal. Such a small error can suggest reproducibility, because this difference is probably caused by human errors, precision of the equipment used to quantify the hydrogen evolution, and variation in the initial conditions, like catalyst mass and glycerol concentration, for example. These results can attest to the reproducibility of the experiments carried out during this work.

4.3 Calcination Temperature

Calcination is a process that is usually required to produce a proper photocatalyst, done under high temperature, for long periods of time, normally in the 300—500 ºC range, for Au/TiO_2 catalysts, or even higher, for 3 to 5 hours. The main objective of the calcination step is the change in the crystalline phase of the semiconductor and the formation or reduction of the metal nanoparticles at the surface of the semiconductor [12].

The crystalline phase is a very important property of the materials that can greatly influence their efficiency, as reported by Wahab et al. [30], whom have shown that there is a clear improvement of the efficiency by the anatase phase, when compared with rutile, as anatase is better at trapping charge carriers in their lattice and has the lowest recombination rate of all of them [30]. Despite anatase being better, the hydrogen production is the best for a mixture of both phases, with anatase being the predominant phase due to the synergistic effect observed, as rutile or brookite can effectively transfer electrons, which were injected into the CB bands by the Au nanoparticles, into the CB of anatase. Due to the lower recombination rates observed in the anatase phase, and the synergistic effect, a mixture of phases seems to be more efficient for the photocatalytic process.

Yudoyono et al. [31] showed that in TiO_2 powders, increasing the calcination temperature causes phase transformation from anatase to brookite. By increasing the temperature from 300 to 600 ºC, the samples showed an increase of the anatase phase and a decrease in the brookite phase, with no rutile phase present [31]. Because the anatase phase is the most efficient, the increments in its total percentage should give better properties to the catalyst, increasing its efficiency and photocatalytic hydrogen production.

It is reported that increasing the temperature, at around 600 ºC, the anatase phase starts changing to rutile [32], which is unfavorable for the hydrogen production, as rutile has a higher charge carriers recombination rate. Calcination temperatures higher than 600 ºC can also have a sintering effect on the nanoparticles, causing poor dispersion and particle agglomeration [12], which reduces the surface active sites; so calcining at higher temperatures can affect the hydrogen production efficiency.

The effect of the calcination temperature was studied for three distinct temperatures and for the non-calcined photocatalyst (only dried): 60 (uncalcined/dried), 300, 450 and 600 ºC. For all of the calcination pre-treatments, the material was calcined for 4 hours at the constant desired temperature. Figure 12 shows the hydrogen production rate evolution curves during 3 h of reaction, as well as the total hydrogen production quantities after 3 hours of reaction.

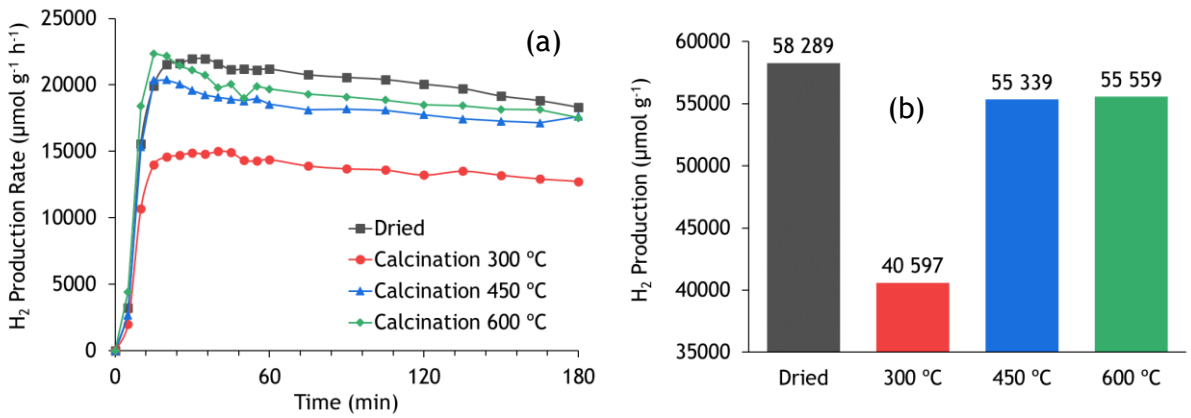

Figure 13 — H_2 production rate (a) and total H_2 production after 180 min of reaction (b) for the different calcination treatments. Conditions: T = 50 ºC; d_p = < 100 µm; $[glycerol]_0$ = 5%(vol); V_{sol} = 300 mL; I = 500 W m^{-2}; [cat] = 0.75 g L^{-1}; Au loading = 2%; pH = 6.39.

From these results, the influence of the calcination step on the catalysts is evident as they all hinder their photocatalytic efficiency improvement. The best performance came from the dried Au/TiO_2 photocatalyst, which had a maximum H_2 production rate of 21 976 µmol g_{cat}^{-1} h^{-1} and a total hydrogen production of 58 289 µmol g_{cat}^{-1} during 3 h of reaction; the worst hydrogen production was verified for the photocatalyst calcined at 300 ºC, with the H_2 production rate peaking at 14 997 µmol g_{cat}^{-1} h^{-1}, totaling a hydrogen production of 40 597 µmol g_{cat}^{-1}, after 3 hours. The three calcined materials, with different calcination pre-treatment, showed an

increasing trend for the hydrogen production, in the chosen temperature interval, tough the major improvement is observed when increasing the calcination temperature from 300 to 450 ºC.

The samples produced in this work use a TiO_2 support composed of 86% of anatase and the rest is rutile, which can explain the behavior of the H_2 production for the calcination temperatures employed (300, 450 and 600 ºC). By increasing the temperature of the calcination pretreatment, the composition of our samples will change, producing brookite phases, which become less and less predominant by increasing the temperature of the calcination, given the growth in the anatase phase.

Calcining at temperatures lower than 400 ºC can hinder the efficiency of the photocatalyst because such low temperatures can lead to incomplete phase transformation, which reduces the efficiency of the photocatalyst, [12] explaining the poor performance of the photocatalyst calcined at 300 ºC. This can also be supported by the probable incomplete phase transformation of the semiconductor, and to the incomplete reduction of Au^{3+} species, which consequently lowers the total surface active sites, hindering the hydrogen production efficiency.

The duration of the precipitation process during preparation is reported to influence the speciation of the Au nanoparticles. Au/TiO_2 catalysts that are dried for a period of less than 2 hours, with no calcination step, are populated by Ti^{3+} and Au^{3+} species at its surface, result from the formation of $Au(OH)_3$ oligomers. Because the Au species are not metallic, they are not expected to give high H_2 productions. Analysis on some Au/TiO_2 samples, prepared through deposition-precipitation, revealed the presence of high concentrations of Ti^{3+} species on the surface of the dried catalyst.

The Ti^{3+} species can reduce the absorbed Au^{3+} species to metallic gold, Au^0, leading to a surface composition of both Au^{3+}/Au^0 and Ti^{3+}/Ti^{4+} species. If the drying step is long enough, at least 12 hours, the Ti^{4+} will reduce the gold almost completely. The extension of the precipitation time, from 2 to 12 hours, enabled the formation of equally sized and highly dispersed gold nanoparticles, contributing to the high H_2 productions [33].

The preparation of our samples proposed a precipitation duration of about the same time as the latter report, 12 hours [33], supporting the presence of Au^0 nanoparticles, and consequently surface active sites, at the surface of the photocatalyst. The material is considered self-doped, eliminating the necessity of an additional calcination step.

In the uncalcined photocatalyst there is an elimination of the problems of the calcination treatment, like gold nanoparticle clustering, particle sintering and poor dispersion, but with the same Au speciation at the surface, Au^0, so the photocatalytic process is expected to be more efficient when the catalyst is self-doped.

In the calcined photocatalysts, these Au^{3+} species will be gradually reduced to Au^0, metallic gold, to provide the necessary surface active sites to conduct the photocatalytic reactions [33]. Because the calcination pretreatments lead to lower production efficiencies, this can also be a result of the calcination duration, that also affects crystallinity, which can influence the gold speciation at the surface, as well as its concentration in comparison to unreduced gold (Au^{3+}).

For the calcinations, the highest temperature, 600 ºC, gave the best performance in terms of total hydrogen production after 3 h of reaction. From the experiments, calcining a sample at a temperature of 600 ºC gives almost the same result as only drying a sample, which could be explained by the presence of similar quantities of Au^0 active sites on both samples. Because the best performance came from the dried sample, all further photocatalysts were not subjected to a calcination step.

4.4 Particle Size

To study the influence of the size of the photocatalyst particle in the overall hydrogen production, two different particle size ranges were studied, <100 µm and 100—200 µm. Figure 13 shows the hydrogen production rate evolution curves during 3 h as well as the total hydrogen production quantities, after 3 hours of reaction. Clearly, different sizes of the photocatalyst lead to drastically different photocatalytic hydrogen production efficiencies. For the lower particle size, of <100 µm, the maximum observed H_2 production rate was 21 976 µmol g_{cat}^{-1} h^{-1}, totaling a hydrogen production of 58 289 µmol g_{cat}^{-1} during the reaction time; for the bigger particles, 100—200 µm, the photocatalytic hydrogen production significantly increased, peaking at a maximum H_2 production rate of 33 713 µmol g_{cat}^{-1} h^{-1}, and a final production of 84 772 µmol g_{cat}^{-1}.

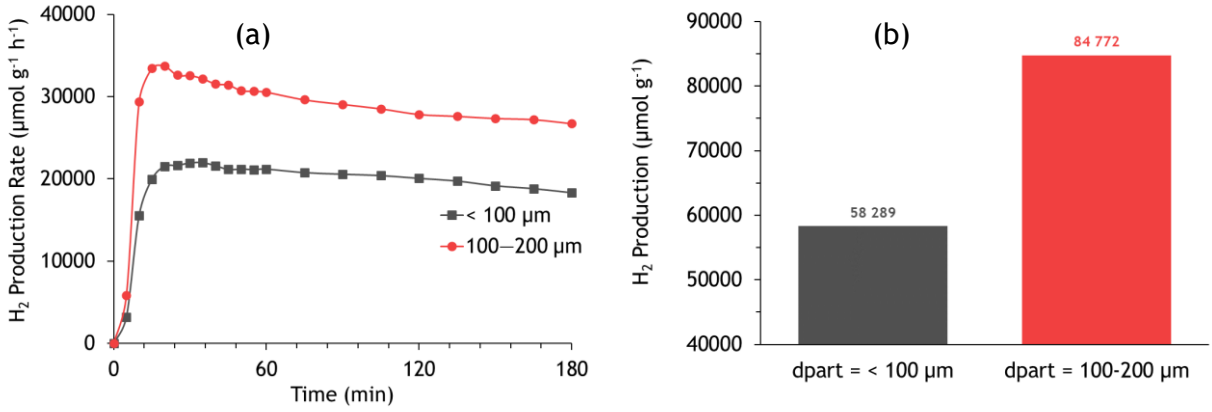

Figure 14 — H_2 production rate (a) and total H_2 production after 180 min of reaction (b) for the different particle sizes. Conditions: T = 50 ºC; [glycerol]$_0$ = 5%(vol); V_{sol} = 300 mL; I = 500 W m^{-2}; [cat] = 0.75 g L^{-1}; Au loading = 2%; pH = 6.39.

One of the factors that can be affecting the efficiency of the lower range of sizes is the suspension turbidity. This property can be defined as the capacity of a solution to disperse and

absorb light, which prevents its transmission in depth, hindering the extent to which the radiation reaches all of the reaction media to activate the photocatalyst.

Sakurai et al. [34] studied the influence of the particle size in an identical catalytic system, Au/TiO_2, for four different sizes, granules and a powder (granules of 450, 125—300, 40—125 μm and a powder of size 5.70 μm) showing a decreasing tendency for hydrogen production when the particle size is increased, for the granules, so that the higher diameter ranges showed almost no hydrogen production, compared to the other samples [34]. This can be further supported by the ratio between the surface area and the volume of the particle, when assuming the particle geometry to be spherical. Indeed, this ratio decreases with the increasing particle diameter, and so there is a decrease in the available surface area, and consequently fewer active sites. Moreover, smaller particles have less problems of internal mass transfer. This contradicts the increasing hydrogen production from <100 to 100—200 μm observed in the experiments of the present work [32]. However, Lin et al. [34] also measured the turbidity of their suspension, for all of their samples and, interestingly, the turbidity values of the samples with higher sizes were all the same, <10 NTU [34], which can explain the best result for the lowest granule size (40—125 μm), because if turbidity is constant, the lowest particle size should therefore reach the best productions. The powder, of average size 5.70 μm, revealed the highest turbidity values, and almost no H_2 production (~17 300 NTU and 0.8 μmol h^{-1}, respectively), showing the negative influence of the turbidity of the suspensions on the photocatalytic hydrogen production.

To better understand the influence of the turbidity of the suspension, measurements with a solution of glycerol (5 vol. %) and the suspended catalyst, with constant agitation to eliminate sedimentation problems as best as possible, were conducted. If the turbidity levels are high, the suspension is considered cloudy, so the incident radiation scatters easily, affecting the light absorption efficiency of the photocatalyst. Turbidity measurements to both particle size suspensions showed a much higher value for the lower size compared to bigger particles: 370 and 70 NTU, respectively. These results indicate that the smaller particle sizes (<100 μm) are better at scattering light and absorb a lower percentage of the incident radiation throughout the suspension, creating a significant cloudiness that inherently disables the full penetration of the radiation. When the photocatalyst is slightly larger, in the 100-200 μm range, the light does not scatter so much, reaching a higher percentage of the reaction media. From our results, one can conclude the prevalence of the influence of the turbidity against particle size because even though the size was smaller, the turbidity levels showed a higher value, affecting the performance.

4.5 Gold Loading

The metal loading is one of the most influential variables in this type of process, affecting, for instance, the total surface active sites, which enable the redox reactions; the Schottky barrier, created by the contact between the metal and the support, hindering the recombination rate of the photoinduced charge carriers (e^-/h^+); the band gap energy, which can be shifted by the deposition of Au; among several others. To evaluate the influence of the gold loading, four different samples with distinct theoretical gold loadings were prepared, namely, 1, 2, 3 and 4 wt.%. Figure 14 shows the hydrogen production rate evolution throughout the reaction time and the total quantity of hydrogen produced during 3 h of reaction.

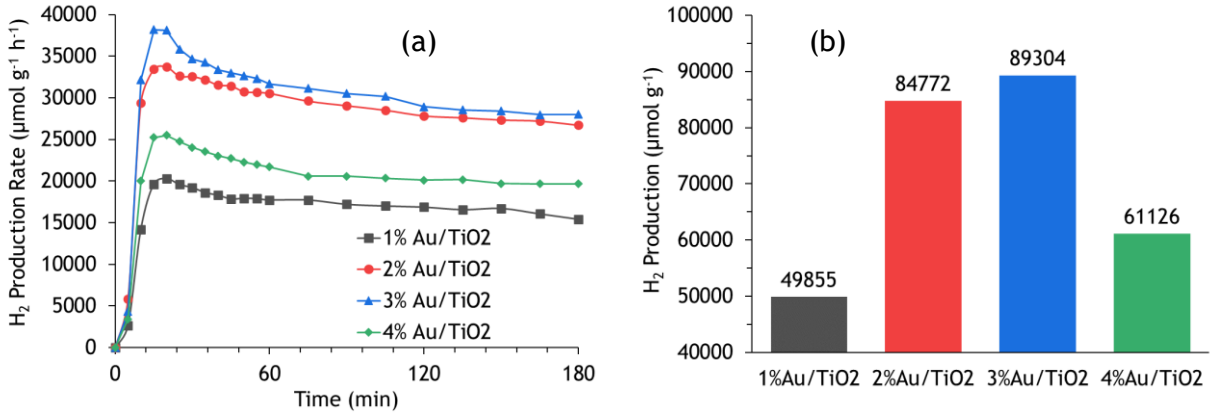

Figure 15 — H_2 production rate (a) and total H_2 production after 180 min of reaction (b) for the different gold loadings. Conditions: T = 50 ºC; d_p = 100-200 μm; $[glycerol]_0$ = 5%(vol); V_{sol} = 300 mL; I = 500 W m^{-2}; [cat] = 0.75 g L^{-1}; pH = 6.38.

From the curves, the 3%Au/TiO_2 sample attained the best results, in terms of performance, with a maximum hydrogen production rate of 38 206 μmol g_{cat}^{-1} h^{-1}, totaling a production of 89 304 μmol g_{cat}^{-1}, after 180 minutes. The photocatalytic hydrogen production followed the order 1% < 4% < 2% < 3%, with the worst performance being observed on the lowest gold loading, 1%, with a maximum rate of H_2 production of 20 314 μmol g_{cat}^{-1} h^{-1}, and a total production of 49 855 μmol g_{cat}^{-1}. For the first three loadings, 1, 2 and 3%, there is a clear increase in the H_2 production (Figure 14), which is a result of the increment in the nominal gold loading. This is in agreement with the results obtained by Méndes-Medrano et al. [35], that observed an increase in the H_2 production when the gold loading as increased from 1 to 2% (468 to 720 μmol g_{cat}^{-1} h^{-1}, with a radiation wavelength of 470 nm).

López-Tenllado et al. [36] revealed a similar rising tendency in hydrogen production from glycerol for the range of gold loadings between 0.5 to 3.0%. They showed that the hydrogen produced by their samples was not linearly proportional to the gold loading [36], further confirming our results, given that the hydrogen productions rose by 70 and 5% by increasing the nominal gold loadings from 1 to 2 and 3 wt.%.

Murdoch et al. [37] found that increasing the Au loading on the sample contributes to the increasing size of the deposited nanoparticles, by gradually broadening the size distribution of the deposited particles. The size of the nanoparticles directly affects the total active sites at the surface, given that they are a limiting factor in terms of photocatalytic efficiency, due to the influence of their concentration on the number of active sites that are available to trigger the desired reactions. Regarding this, the total active surface sites are increased with the reduction of the gold particle size deposited at the surface of the photocatalyst due to the increase in the available area for light absorption and the increase of the total perimeter of the metal particle at the surface, as well as the strong contact between the nanoparticles and the support, contributing to the electron transitions between them. Smaller gold nanoparticles are therefore beneficial to the photocatalytic hydrogen production process, due to the higher perimeter of the contact site of the metal, which are known to be the preferential sites of adsorption and consequent glycerol degradation.

Lin et. al [38] state that for the hemispherical gold nanoparticles the hemispherical surface area (s_h), interfacial contact area (s_c) and interfacial perimeter (p_i) can relate to the area of the material where light is absorbed (LSPR phenomena), the electron transfer mechanisms and the interfacial active sites, respectively [38]. The total interfacial active sites are the most important given that they are responsible for the degradation of the sacrificial agent in the solution, so optimizing the interfacial perimeter is advantageous.

Indeed, for their samples, the best results for all three parameters came from the smallest Au nanoparticles, 2.8 nm, which showed an interfacial perimeter ratio of nearly 50:12:1 (2.8, 6.2 and 32 nm, respectively), so these nanoparticles optimize the photocatalytic efficiency. This can corroborate the necessity of depositing the smallest nanoparticles possible, in order to optimize the interfacial perimeter and to increase the total surface active sites. It is expected that our samples will have hemispherical gold particles smaller than 4 nm, as reported by Haruta [21], so their efficiency is expected to be almost optimal gold nanoparticle sizing.

The emission spectra of the radiation source can also dictate the efficiency of the photocatalyst, especially in gold doped semiconductors, because of the LSPR properties of the gold nanoparticles at the surface of the photocatalyst, that strongly help the hot electron injection from the gold nanoparticles into the conduction band of the TiO_2. Because there is a higher gold content at the surface of the photocatalyst for higher loadings, the absorption of visible light by the Au nanoparticles should increase, consequently enhancing the injection rate of photogenerated species to the conduction band of TiO_2, which increases the number of available charge carriers to undergo photocatalytic reactions.

Au/TiO_2 has a LSPR band in the 400-650 nm range, with peak wavelengths of around 550 nm, [37] so it is expected that excitation at this wavelength could increase the visible light

absorption of the catalysts. This is indeed verified by our results, that using a lamp that emits in the visible light range (with a particular peak around 550 nm, see Annex C) helps the efficiency of the gold-driven charge carrier transitions, due to the strong LSPR effects. The radiation wavelength range of the lamp used in this work could also explain this increase in the H_2 production, given that it emits mostly in the visible range, with peaks at 380, 410, 440, 550 and 580 nm (Annex C). The peaks of 550 and 580 nm contribute to the LSPR effect of gold by light absorption, helping gold nanoparticles trap energy carriers to trigger photocatalytic reactions [35][39]. The gold surface coverage can also severely affect the photocatalytic efficiency if it is too high, given that gold particles obstruct the TiO_2 exposed sites, which consequently reduces the light absorption capacity of the catalyst, due to the light absorption characteristics of both TiO_2 and Au, which absorb mostly UV and visible light, respectively. If the Au loading is too high, it can cause excessive gold deposition and consequent excessive surface coverage, limiting the light absorption to the visible light absorption by the Au nanoparticles, hindering the UV absorption of TiO_2, which directly affects the hydrogen production capacity of the catalyst. This could be investigated further by some characterization techniques to obtain the real Au loading on the samples and the metal coverage (dispersion) and size distribution.

The results found by both Lin et al. [38] and Murdoch et al. [37] show that the interfacial perimeter is responsible for the total active sites on the catalyst; that by increasing the loading, the distribution of the nanoparticle size is broadened, and the average size is therefore increased. This explains the decrease in H_2 production efficiency by increasing the dopant's loading from 3 to 4%, similarly to the work from Jovic et al. [40], whom have noticed that when the loading increased from 3 to 4%, the H_2 production decreased, and the mean Au particle size increased. The worse performance could mean that a 4% nominal gold loading can already be contributing to the diminishing of the total interfacial active sites by over-crowding the surface of the photocatalyst, which decreases the total UV absorption [37]. The decrease of the reaction rate at higher Au sizes is therefore most likely a geometric effect rather than an electronic one, the critical factor is the inter-cluster distance of the gold nanoparticle clusters on the surface of the TiO_2 [41].

4.6 Initial pH

The initial pH of the solution has a strong influence on the overall photocatalytic performance, affecting the photocatalyst agglomeration and the glycerol adsorption at the surface of the photocatalyst, primarily, but other factors are also subject to change [39].

To evaluate the influence of the initial pH value of the glycerol solution, experiments using different initial pH values were conducted, for pH values of 5.0, 6.39 (natural pH value of the

glycerol solution), 8.0 and 10.0. Figure 15 shows the hydrogen production rate evolution and total production of all experiments, during the 180 minutes of reaction.

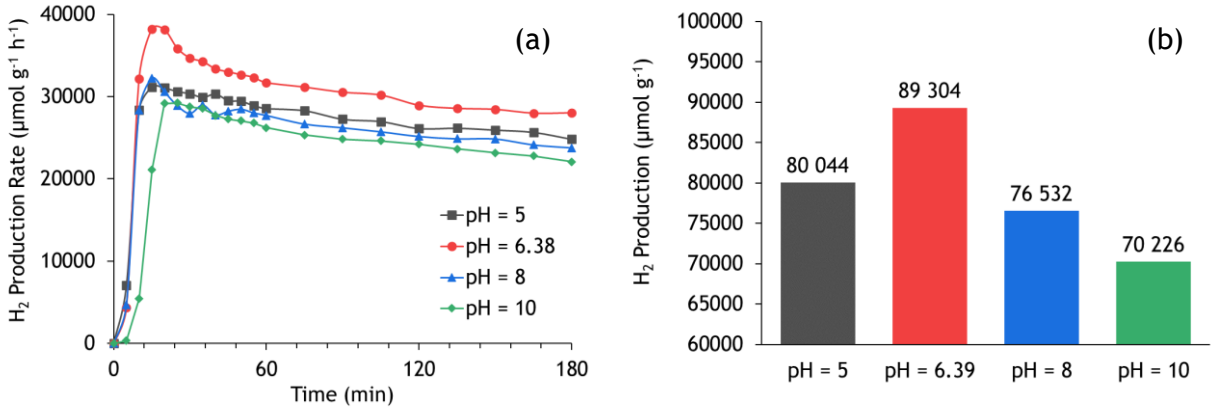

Figure 16 — H_2 production rate (a) and total H_2 production after 180 min of reaction (b) for the different initial pH experiments. Conditions: T = 50 ºC; d_p = 100—200 μm; $[glycerol]_0$ = 5%(vol); V_{sol} = 300 mL; I = 500 W m^{-2}; [cat] = 0.75 g L^{-1}; Au loading = 3%.

Firstly, it is rather apparent that all of the chosen pH values can be used to conduct the experiments, given that all of them produce H_2 to some extent. Between all of the experiments, the initial pH value that was found to be the optimal was the natural pH of the prepared glycerol solution, with a pH of 6.39, with a maximum H_2 production rate of 38 206 μmol g_{cat}^{-1} h^{-1}, and a final production of 89 304 μmol g_{cat}^{-1}. The worst performance was when the initial pH value was 10, with a maximum H_2 production rate of 29 223 μmol g_{cat}^{-1} h^{-1}, and a final production of 70 226 μmol g_{cat}^{-1}.

The initial pH of the solution can indeed influence the surface charges of the photocatalyst, if this pH value is either lower or higher than the point of zero charge of the catalyst (pHpzc), being one of the most important effects in the photocatalytic efficiency. This property of the photocatalyst dictates how the molecules present in solution adsorb at its surface, given their speciation. When the pH value of the solution transits through the pHpzc point, the surface reactions occurring at the interface between the bulk and the surface are changed, and the mechanism is altered.

The interactions that happen between the catalyst and the sacrificial molecules are important since the glycerol molecules adsorb at the surface mainly through hydrogen bonding with the existent surface hydroxyl groups. If the pH is lower than the pHpzc, the dominating ionic species in solution will be H^+ ions; if the pH is higher than the pHpzc, OH^- ions are now the most prevalent species in the solution. This is described in the following equations, that depict the surface reactions, for both pH levels, and based on the equations, it is inferred that the charges on the surface are different, which alters the mechanism of adsorption of the glycerol molecules, in both pH regimens, following Equations (5) and (6) [39].

$$Ti^{IV}{-}OH + H^+ \rightarrow Ti^{IV}{-}OH_2^+ \qquad pH < pHpzc\ 2H+ \text{->}\ H2 \qquad (5)$$

$$Ti^{IV}{-}OH + OH^- \rightarrow Ti^{IV}{-}O^- + H_2O \qquad pH > pHpzc \qquad (6)$$

Below the pHpzc (pH < 6.38), the surface is positively charged, creating electrostatic repulsion forces between the surface and the H^+ ions on the solution, which affects the photocatalytic efficiency [39]. TiO_2 particles agglomerate for acidic solutions, leading to a lower percentage of surface area exposed for glycerol adsorption, decreasing the harvesting of the incident photons by the catalyst.

When the pH of the solution is above the pHpzc of the catalyst, the surface is now negatively charged, creating repulsing forces between the surface hydroxyl groups and the glycerol molecules given their negative charge (pKa = 14.4), affecting the glycerol adsorption on to the h^+_{VB}. The photogenerated species, i.e. the electron-hole pair, are also more likely to recombine in the basic range due to the negative charges on the surface, inhibiting the transition of the electrons to the conduction bands [39].

The most efficient pH value for the solution is therefore the natural pH of the glycerol solution, 6.38, which neutralizes the charges at the photocatalyst's surface, eliminating the repulsion forces created by both acidic and basic initial solutions and enhancing the migration of the generated charge carriers, increasing the efficiency of the process. Vaiano and Iervolino [42] also corroborated these results, for another catalyst system, Cu/ZnO. Such study shows the negative influence of the pH in very acidic (or basic) solutions, compared to the natural pH of the glycerol solution, which they attributed to the glycerol adsorption, charges and band gap position of the photocatalyst, hinting that the adsorption of the glycerol molecules is dictated by the pH of the solution [42]. These results attest to the bad performances of the initial pH values of 5, 8 and 10.

To confirm these assumptions, the pHpzc of the photocatalyst sample was measured and verified to be 6.38 (more information on Annex B), close to the natural pH of the water-glycerol solution, 6.39, measured at the beginning of every conducted experiment. As it can be seen, the pH value that performed the best was indeed the natural pH of the solution, confirming that neutralizing the charges at the surface of the photocatalyst is beneficial to the overall photocatalytic efficiency, due to the hindering of both the repulsion forces created between the solution and the photocatalyst, as well as the recombination of the photogenerated species. This is also economically advantageous because choosing the natural pH of the prepared solutions eliminates the necessity of adjusting the pH prior to the experiments, with additional chemicals that are unnecessary.

The pH of the solution is however not constant throughout the reaction duration, virtue of the constant degradation and formation of both glycerol and its intermediates, which are also

adsorbed at the surface of the photocatalyst [12]. In this work, the pH value of the solution was always measured at the beginning and end of every experiment, to register the absolute change in pH during the 180 minutes of reaction. Indeed, from every experiment, the average final pH was 3.27 ± 0.22. The final pHs for the different initial pH solutions, of 5, 6.38, 8 and 10, were 3.47, 3.45, 3.15 and 3.09, respectively. This can be explained by the formation of several carboxylic acids in the solution, as well as the formation of other intermediates, which lower the pH value of the solution, confirming the degradation of the initial glycerol solution [12].

This pH change can also help explaining the observed rate of hydrogen production decreasing throughout the duration of the reactions, given the poor rate of adsorption of the molecules in the solution after the pH starts to decrease, to levels lower that the pHpzc. To further analyze if this aspect is heavily affecting the overall production of H_2, it would be necessary to conduct experiments with a pH controller, or a buffer, to maintain it at the initial value, causing no variations, to see if the H_2 evolution would reach a plateau and stabilize, or even increase during the reactions.

4.7 Reaction Temperature

The reaction temperature is one of the most important variables in almost all chemical reactions, and can severely improve the efficiency of the process. To study the influence of the temperature of the reaction, three tests were performed at three different temperatures: 50, 70 and 90 ºC.

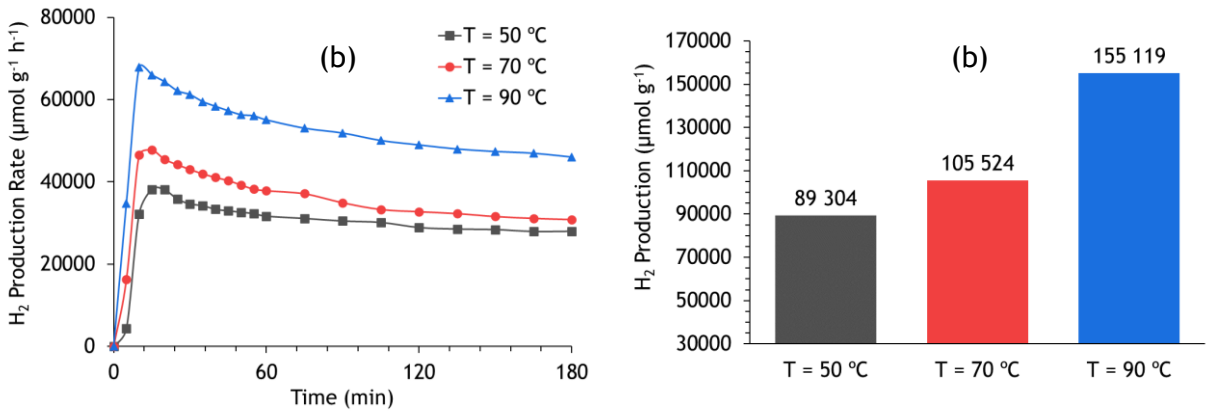

Figure 17 — H_2 production rate (a) and total H_2 production after 180 min of reaction (b) for the different reaction temperatures. Conditions: pH = 6.39; d_p = 100—200 µm; $[glycerol]_0$ = 5%(vol); V_{sol} = 300 mL; I = 500 W m^{-2}; [cat] = 0.75 g L^{-1}; Au loading = 3%.

Figure 16 shows the evolution of the hydrogen production rate, and the total hydrogen production, for all of the experiments. From these results, there was a clear increase in the hydrogen production with an increase in the reaction temperature, which was to be expected, given the well-known improvement of the kinetics by increasing the temperature. Results show

the best temperature, in terms of production, to be 90 ºC, with a maximum rate of hydrogen production of 67 873 µmol g_{cat}^{-1} h^{-1}, totaling a final production, after 3 hours, of 155 119 µmol g_{cat}^{-1}. The lowest value was observed when the temperature was kept at 50 ºC, with a maximum rate of hydrogen production of 38 207 µmol g_{cat}^{-1} h^{-1}, totaling a final production of 89 304 µmol g_{cat}^{-1}.

Temperature is largely known to be one of the most influential variables in any chemical reaction, due to the increase in the kinetics with a temperature increase ($r_{H2} \propto T$). This can be explained by the increase in the kinetic constant (k), by an increase in temperature (T), following Equation (7) – Arrhenius law (wherein E_a is the activation energy, k_0 the pre-exponential factor and R the ideal gas constant).

$$k = k_0 \, e^{-\frac{E_a}{RT}} \tag{7}$$

Based solely on this equation, it is expected that the H_2 production rate will increase as a result of an increase of the temperature, which was indeed observed, for the temperature range in study, in the order r_{H2} (50 ºC) < r_{H2} (70 ºC) < r_{H2} (90 ºC).

4.8 Long-Term Reaction

The total duration of the reaction was studied for two durations, 3 hours, the normal reaction time used for all of the conducted experiments, and 26 hours, to conduct a longer experiment, to see the influence it has on the process itself. In this experiment, the initial conditions were the best results for each optimization variable, 3%Au/TiO_2 (100—200 µm) at 90 ºC, with the glycerol solution at 5% vol and initial pH of 6.38. In this run, both CO and CO_2 were also quantified.

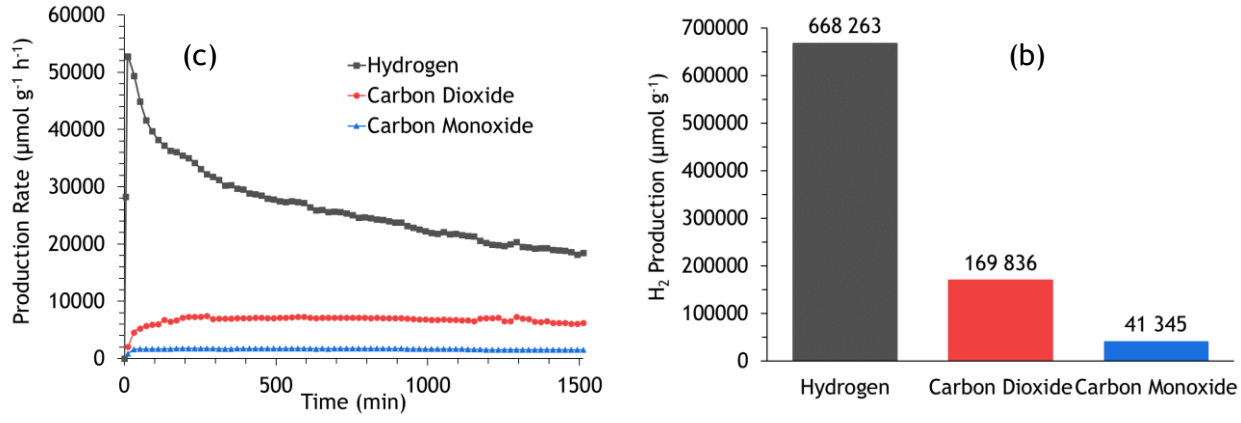

Figure 18 — Production rate (a) and total H_2 production after 26 h of reaction (b) for H_2, CO_2 and CO. Conditions: T = 90 ºC; d_p = 100—200 µm; pH = 6.39; [glycerol]$_0$ = 5%(vol); V_{sol} = 300 mL; I = 500 W m^{-2}; [cat] = 0.75 g L^{-1}; Au loading = 3%.

Figure 17 shows the hydrogen evolution curve for the 26-hour long experiment, as well as its final production value. The maximum H_2 production rate was observed to be 52 753 μmol g_{cat}^{-1} h^{-1}, after 15 minutes, totaling a production of 668 263 μmol g_{cat}^{-1}. Both CO and CO_2 stabilized around values of 1 635 and 7 578 μmol g_{cat}^{-1} h^{-1}, for their production rate, totaling production quantities of 41 345 and 169 836 μmol g_{cat}^{-1}, respectively.

The long run was performed to better understand the evolution of the hydrogen production through time. From these results, it is inferable that the hydrogen production will always decrease, even for longer reaction durations. The maximum production rate appears around the 10 to 15-minute mark, which can be explained by the fast glycerol consumption at the beginning, when the photocatalyst is activated, allowing for the adsorption of glycerol molecules and their consequent degradation. The photocatalytic glycerol conversion into hydrogen is not a single step reaction, given the formation of several intermediary species that can also be adsorbed at the surface or suffer degradation by other species in solution. The production rate will decrease for the rest of the reaction, after the peak, with an initial accentuated decrease rate, for around 200 minutes, and then the production rate has a smoother decreasing rate.

From the results, and the peak rate observed at the beginning of every single reaction, it is probable that glycerol is preferentially dehydrogenated rather than dehydrated, because dehydrogenation forms hydrogen (dehydration forms H^+ and H_2O), which can explain the fast initial H_2 production. After several hours, the rate is still decreasing, albeit a lot slower, which can be a result of the adsorbed intermediary species, being then degraded into gradually smaller molecules, resulting in the formation of 3 gases, H_2, CO_2 and CO. The glycerol molecules are also being consumed throughout the reaction, and the pH is also not constant (as referenced in Subchapter 4.5), which lowers the efficiency of the process, further explaining the decreasing tendency in the H_2 production rate.

It is also worth noting that in the Subchapters 4.6 and 4.7, the results from the long duration test and the 90 ºC test were different, in terms of production, even at the same conditions, as confirmed by their maximum production rate, 52 753 (Sub. 4.6) and 67 873 μmol g_{cat}^{-1} h^{-1} (Sub. 4.7), which is unexpected. The experiments were quantified with another gas chromatograph, which can also be introducing some error. This could probably be a result of the sample storage methods, which can change the properties of the catalysts, but other factors might also be affecting the stability of the catalyst [43]. Indeed, Wu et al. [43] showed that, for the catalyst Au/TiO_2, prepared by deposition-precipitation in the dark, similar to this work, even an increase of 15 days in storage, the catalyst could reduce its catalytic efficiency by a factor of 6.5, when the catalyst loading is 0.7%. It was shown that for all of the catalysts, the catalytic efficiency is always hindered by storage in air containers, at temperatures higher than 50 ºC [43].

5 Conclusion

Photocatalysis arose as one of the most efficient hydrogen production methods, creating pressure to drive efforts to further develop and improve this technology, in order to establish a safe, sustainable and clean technology to produce the future's energy vector. This process usually aims for the utilization of solar power as radiation source, to increase the process sustainability, coupled with the intent to use waste as raw-material for the conversion reactions that take place.

The feasibility of this process is based upon the necessary irradiation, which is a direct consequence of the employment of a semiconductor as a photocatalyst. But the extent to which hydrogen is produced is a product of the interconnectivity between the influence of some variables to this process, like temperature, pH, method of photocatalyst preparation, among several others. Aiming for the best process parameters possible, a detailed parametric study was conducted to assess the effect of the calcination treatment, photocatalyst particle size, surface gold loading, initial pH, and reaction temperature, changing one variable at a time.

The calcination treatment was proven to be ineffective in terms of optimization of the H_2 production, as calcining the samples lead, in all cases, to a decrease in the overall hydrogen production. The simply dried material performed the best, with a maximum H_2 production rate of 21 976 μmol g_{cat}^{-1} h^{-1} and a total hydrogen production (after 3 h) of 58 289 μmol g_{cat}^{-1}.

Following calcination, the particle sizing influence was studied, revealing the best particle sizing to be the highest range studied, of 100—200 μm, due to the higher radiation percentage that penetrates the solution. Indeed, with the higher particle sizes, the photocatalytic hydrogen production significantly increased, with a maximum H_2 production rate of 33 713 μmol g_{cat}^{-1} h^{-1}, and a final production of 84 772 μmol g_{cat}^{-1}.

The gold loading was then studied, to search for the best loading possible. This confirmed a clear improvement in the hydrogen evolution curves for the sample with a nominal gold loading of 3%, as opposed to the other loadings of 1, 2 and 4%, with a maximum hydrogen production rate of 38 206 μmol g_{cat}^{-1} h^{-1}, totaling a production of 89 304 μmol g_{cat}^{-1}, after the 3 hours.

The initial solution pH value was the variable studied next. This set of experiments revealed a clear improvement of the process when the natural pH of the glycerol solutions was used. The other initial pH values (5, 8 and 10) were found to be detrimental to the overall hydrogen evolution, mainly due to the glycerol adsorption properties and surface charges of the photocatalyst system in use.

The temperature of the reaction was then studied, showing an expected increase in production with the temperature increments performed. The best temperature was found to be 90 ºC, the highest temperature studied, with a maximum rate of hydrogen production of 67 873 µmol g_{cat}^{-1} h^{-1}, totaling a final production, after 3 hours, of 155 119 µmol g_{cat}^{-1}.

The final conducted experiment tested the influence of the reaction duration on the H_2 production, extending the total time to 26 hours, with a maximum rate of 52 753 µmol g_{cat}^{-1} h^{-1} and a total production of 668 263 µmol g_{cat}^{-1}. In this experiment, both CO and CO_2 reached stable values after around 3 hours of 1 635 and 7 578 µmol g_{cat}^{-1} h^{-1}, for their production rates, with total production quantities of 41 345 and 169 836 µmol g_{cat}^{-1}, respectively.

In conclusion, there is a clear set of operation conditions, from the preparation method of the catalyst until the conditions and variables tested, that lead to highly efficient materials that can conduct photocatalytic reactions with high H_2 production rates and production quantities. It was found through the parametric study that both the calcination pre-treatment and the pH adjustment of the initial solution are unnecessary steps, which can be eliminated from the process. On the other hand, optimal values were found for all of the other variables namely, temperature, gold loading and particle size.

These results confirm the possibility of using photocatalysis to produce clean hydrogen, at high quantities, by using by-product waste streams, from the biodiesel industry. This process is considerably effective and highly efficient, as a result of the employment of an Au doped TiO_2 as a photocatalyst system, as it is conducted under mild conditions, in terms of temperature and pressure, but it also discards extra steps (calcination and pH adjustments), helping the process economically and environmentally.

6 Assessment of the work done

6.1 Objectives Achieved

This process was proven to be very efficient in the production of hydrogen from aqueous glycerol solutions, by using as radiation source a simulated UV and visible light lamp, which was the very first objective of this work. After confirming the feasibility of the process, the process variables were then studied carefully to choose the optimization route to be followed.

The optimization of a range of variables was the other main objective, in order to reach the best H_2 production values possible. Optimal values were found for all of the variables in study, and for two of them, the results show that their influence is detrimental: the calcination pre-treatment was proven unnecessary and the initial pH solution adjustment was also found to be pointless, as the natural pH of the solutions gave the best performance. This reduced the process steps, and helps at both the economic and environmental level.

6.2 Future Work Suggestions

To further improve the advancements made in this work, the following premises are proposed:

i. All of the samples should be characterized to better understand the physical real properties of the catalyst in use, through methods like TEM, FT-IR, XPS, XRD and EXAFS. This could help reducing the hypothetic assumptions made about the real gold loading of the samples and maybe providing a clear reason for this variability (theoretical vs. real loading);
ii. The preparation method could be further improved to produce better samples by changing the basic agent responsible for the pH control of the preparation environment. Urea is a great substitution, as it is found to help gradually precipitate the gold precursor on the surface, as opposed to the NaOH injections;
iii. Preparations of bimetallic coupled semiconductors could be beneficial for the process, as they are known to be the product of the advantages of both the cocatalysts. Based on the literature, both Pt, Ag and Ru can be great contenders, for example. Ag is interesting because like Au it possesses a LSPR effect, which is known to be beneficial to the process.
iv. The sacrificial agent in use could also be a target of optimization: The concentration in solution, which was hereby fixed at 5%, can be changed and thoroughly studied for this catalyst system. The nature of the sacrificial initial solution can also be subject to study, by creating a mixture of other efficient hole scavengers, to possibly produce more hydrogen and study the influence of the sacrificial mixture, to find which is preferentially oxidized. Studies on the raw and crude glycerol from biodiesel waste streams could also be

performed, to see how the composition affects the efficiency of the process, and then tune the process parameters to optimize the hydrogen production from these streams;

v. The reaction media is a mixture of intermediaries at unknown concentrations through time, and by retrieving aliquot samples of the reactional media the components could be analyzed by liquid phase chromatography (HPLC), to try to establish the reaction network.

vi. The radiation system could also be altered to try to study the influence of the lamp type, intensity and even the coupling of several lights, that can perhaps enhance the production by elevating the total radiation emission and consequent absorption.

7 References

[1] H. Ritchie and M. Boser, “CO2 and Greenhouse Gas Emissions.” 2020. [Online]. Available: https://ourworldindata.org/co2-and-other-greenhouse-gas-emissions

[2] International Energy Agency, “Global energy sector CO2 emissions reductions by measure in the Sustainable Development Scenario relative to the Stated Policies Scenario – Charts – Data & Statistics.” [Online]. Available: https://www.iea.org/data-and-statistics/charts/global-energy-sector-co2-emissions-reductions-by-measure-in-the-sustainable-development-scenario-relative-to-the-stated-policies-scenario

[3] M. Gérard, F., van Nuffel, L., Smit, T., Yearwood, J., ČErný, O., Michalski, J., & Altmann, “Opportunities for Hydrogen Energy Technologies Considering the National Energy & Climate Plans | www.fch.europa.eu.” 2020. [Online]. Available: https://www.fch.europa.eu/publications/opportunities-hydrogen-energy-technologies-considering-national-energy-climate-plans

[4] Eurostat, “Renewable energy statistics - Statistics Explained.” 2021. [Online]. Available: https://ec.europa.eu/eurostat/statistics-explained/index.php?title=Renewable_energy_statistics

[5] J. Adolf, C. Balzer, J. Louis, U. Schabla, and M. Fischedick, “Shell Hydrogen Study Energy of the Future? Sustainable Mobility through Fuel Cells and H2.” 2017. doi: 10.13140/RG.2.2.31848.57604.

[6] International Energy Agency, “Hydrogen – Analysis.” 2020. [Online]. Available: https://www.iea.org/reports/hydrogen

[7] World Energy Council", “Hydrogen - Industry as Catalyst,” World Energy Council, 2019. [Online]. Available: http://www.wereldenergieraad.nl/wp-content/uploads/2019/02/190207-WEC-brochure-2019-A4.pdf

[8] International Energy Agency, “Hydrogen - Fuels & Technologies.” 2020. [Online]. Available: https://www.iea.org/fuels-and-technologies/hydrogen

[9] International Energy Agency, “The Future of Hydrogen – Analysis.” 2019. [Online]. Available: https://www.iea.org/reports/the-future-of-hydrogen

[10] Secretaria de Estado Adjunta e da Energia, “EN-H2 Estratégia Nacional para o Hidrogénio.” 2020. [Online]. Available: https://participa.pt/pt/consulta/en-h2-estrategia-nacional-para-o-hidrogenio

[11] M. Chatzimarkakis, J., Levoyannis, C., & Wouters, F. (2021, "Hydrogen Europe | H2: enabling a zero-emission society." 2021. [Online]. Available: https://www.hydrogeneurope.eu/wp-content/uploads/2021/04/2021.04_HE_Hydrogen-Act_Final.pdf

[12] M. R. Karimi Estahbanati, M. Feilizadeh, F. Attar, and M. C. Iliuta, "Current developments and future trends in photocatalytic glycerol valorization: process analysis," *Reaction Chemistry & Engineering*, vol. 6, no. 2, pp. 197–219, 2021, doi: 10.1039/d0re00382d.

[13] Y. Shen *et al.*, "Promotion Mechanisms of Au Supported on TiO2 in Thermal- and Photocatalytic Glycerol Conversion," *The Journal of Physical Chemistry C*, vol. 123, no. 32, pp. 19734–19741, 2019, doi: 10.1021/acs.jpcc.9b05475.

[14] International Energy Agency, "Transport biofuels – Renewables 2020 – Analysis." 2020. [Online]. Available: https://www.iea.org/reports/renewables-2020/transport-biofuels

[15] X. Xing, S. Tang, H. Hong, and H. Jin, "Concentrated solar photocatalysis for hydrogen generation from water by titania-containing gold nanoparticles," *International Journal of Hydrogen Energy*, vol. 45, no. 16, pp. 9612–9623, 2020, doi: 10.1016/j.ijhydene.2020.01.197.

[16] J. Figueiredo, M. M. Pereira, and J. Faria, *Catalysis from Theory to Application: An Integrated Course*. Universidade de Coimbra, 2008.

[17] E. Kowalska, S. Rau, and B. Ohtani, "Plasmonic Titania Photocatalysts Active under UV and Visible-Light Irradiation: Influence of Gold Amount, Size, and Shape," *Journal of Nanotechnology*, vol. 2012, pp. 1–11, 2012, doi: 10.1155/2012/361853.

[18] F. Amano, M. Nakata, A. Yamamoto, and T. Tanaka, "Rutile titanium dioxide prepared by hydrogen reduction of Degussa P25 for highly efficient photocatalytic hydrogen evolution," *Catal. Sci. Technol.*, vol. 6, no. 14, pp. 5693–5699, 2016, doi: 10.1039/C6CY00296J.

[19] E. Baranowska-Wójcik, D. Szwajgier, P. Oleszczuk, and A. Winiarska-Mieczan, "Effects of Titanium Dioxide Nanoparticles Exposure on Human Health—a Review," *Biological Trace Element Research*, vol. 193, no. 1, pp. 118–129, 2019, doi: 10.1007/s12011-019-01706-6.

[20] R. Zanella, L. Delannoy, and C. Louis, "Mechanism of deposition of gold precursors onto TiO2 during the preparation by cation adsorption and deposition–precipitation

with NaOH and urea," *Applied Catalysis A: General*, vol. 291, no. 1–2, pp. 62–72, 2005, doi: 10.1016/j.apcata.2005.02.045.

[21] M. Haruta, "Size- and support-dependency in the catalysis of gold," *Catalysis Today*, vol. 36, no. 1, pp. 153–166, 1997, doi: 10.1016/s0920-5861(96)00208-8.

[22] W.-T. Chen, A. Chan, Z. H. N. Al-Azri, A. G. Dosado, M. A. Nadeem, and D. Sun-Waterhouse, "Effect of TiO2 polymorph and alcohol sacrificial agent on the activity of Au/TiO2 photocatalysts for H2 production in alcohol–water mixtures," *Journal of Catalysis*, vol. 329, pp. 499–513, 2015, doi: https://doi.org/10.1016/j.jcat.2015.06.014.

[23] M. Yasuda, T. Matsumoto, and T. Yamashita, "Glycerol as a Superior Electron Source in Sacrificial H2 Production over TiO2 Photocatalyst," *Glycerine Production and Transformation - An Innovative Platform for Sustainable Biorefinery and Energy*, 2019, doi: 10.5772/intechopen.85810.

[24] R. Singh and S. Dutta, "A review on H2 production through photocatalytic reactions using TiO2/TiO2-assisted catalysts," *Fuel*, vol. 220, pp. 607–620, 2018, doi: 10.1016/j.fuel.2018.02.068.

[25] F. J. Méndez, A. González-Millán, and J. A. García-Macedo, "A new insight into Au/TiO2-catalyzed hydrogen production from water-methanol mixture using lamps containing simultaneous ultraviolet and visible radiation," *International Journal of Hydrogen Energy*, vol. 44, no. 29, pp. 14945–14954, 2019, doi: 10.1016/j.ijhydene.2019.04.131.

[26] Z.-W. Cheng, L. Feng, J.-M. Chen, J.-M. Yu, and Y.-F. Jiang, "Photocatalytic conversion of gaseous ethylbenzene on lanthanum-doped titanium dioxide nanotubes," *Journal of Hazardous Materials*, vol. 254, pp. 354–363, 2013, doi: 10.1016/j.jhazmat.2013.03.037.

[27] S. M. N. Jeghan, N. Kim, and G. Lee, "Mo-incorporated three-dimensional hierarchical ternary nickel-cobalt-molybdenum layer double hydroxide for high-efficiency water splitting," *International Journal of Hydrogen Energy*, vol. 46, no. 43, pp. 22463–22477, 2021, doi: https://doi.org/10.1016/j.ijhydene.2021.04.071.

[28] B. Gupta, A. A. Melvin, T. Matthews, S. Dash, and A. K. Tyagi, "TiO 2 modification by gold (Au) for photocatalytic hydrogen (H 2) production," *Renewable and Sustainable Energy Reviews*, vol. 58, pp. 1366–1375, 2016, doi: 10.1016/j.rser.2015.12.236.

[29] N. Fajrina and M. Tahir, "A critical review in strategies to improve photocatalytic water splitting towards hydrogen production," *International Journal of Hydrogen Energy*, vol. 44, no. 2, pp. 540–577, 2019, doi: 10.1016/j.ijhydene.2018.10.200.

[30] A. K. Wahab, S. Ould-Chikh, K. Meyer, and H. Idriss, "On the 'possible' synergism of the different phases of TiO2 in photo-catalysis for hydrogen production," *Journal of Catalysis*, vol. 352, pp. 657–671, 2017, doi: https://doi.org/10.1016/j.jcat.2017.04.033.

[31] G. Yudoyono *et al.*, "Effect of calcination temperature on the photocatalytic activity of TiO2 powders prepared by co-precipitation of TiCl3," *AIP Conference Proceedings*, vol. 1725, no. 1, p. 20099, 2016, doi: 10.1063/1.4945553.

[32] G. Kavei, A. Nakaruk, and C. C. Sorrell, "Equilibrium State of Anatase to Rutile Transformation for Titanium Dioxide Film Prepared by Ultrasonic Spray Pyrolysis Technique," *Materials Sciences and Applications*, vol. 02, no. 06, pp. 700–705, 2011, doi: 10.4236/msa.2011.26096.

[33] J. B. Priebe *et al.*, "Solar Hydrogen Production by Plasmonic Au–TiO2 Catalysts: Impact of Synthesis Protocol and TiO2 Phase on Charge Transfer Efficiency and H2 Evolution Rates," *ACS Catalysis*, vol. 5, no. 4, pp. 2137–2148, 2015, doi: 10.1021/cs5018375.

[34] H. Sakurai, M. Kiuchi, C. Heck, and T. Jin, "Hydrogen evolution from glycerol aqueous solution under aerobic conditions over Pt/TiO2and Au/TiO2granular photocatalysts," *Chemical Communications*, vol. 52, no. 93, pp. 13612–13615, 2016, doi: 10.1039/c6cc08319f.

[35] M. G. Méndez-Medrano *et al.*, "Surface Modification of TiO2 with Au Nanoclusters for Efficient Water Treatment and Hydrogen Generation under Visible Light," *The Journal of Physical Chemistry C*, vol. 120, no. 43, pp. 25010–25022, Nov. 2016, doi: 10.1021/acs.jpcc.6b06854.

[36] F. J. López-Tenllado *et al.*, "A comparative study of hydrogen photocatalytic production from glycerol and propan-2-ol on M/TiO 2 systems (M=Au, Pt, Pd)," *Catalysis Today*, vol. 280, pp. 58–64, 2017, doi: 10.1016/j.cattod.2016.05.009.

[37] M. Murdoch *et al.*, "The effect of gold loading and particle size on photocatalytic hydrogen production from ethanol over Au/TiO2 nanoparticles," *Nature Chemistry*, vol. 3, no. 6, pp. 489–492, 2011, doi: 10.1038/nchem.1048.

[38] L. Lin, Q. Zhong, Y. Zheng, Y. Cheng, R. Qi, and R. Huang, "Size effect of Au nanoparticles in Au-TiO2-x photocatalyst," *Chemical Physics Letters*, vol. 770, p. 138457, 2021, doi: 10.1016/j.cplett.2021.138457.

[39] T. W. P. Seadira, S. J. Baloyi, C. M. Masuku, and M. S. Scurrell, "Solar photocatalytic hydrogen production from glycerol reforming using ternary Cu/THS/Graphene," *IOP Conference Series: Materials Science and Engineering*, vol. 655, p. 12049, 2019, doi: 10.1088/1757-899x/655/1/012049.

[40] V. Jovic, W.-T. Chen, D. Sun-Waterhouse, M. G. Blackford, H. Idriss, and G. I. N. Waterhouse, "Effect of gold loading and TiO2 support composition on the activity of Au/TiO2 photocatalysts for H2 production from ethanol–water mixtures," *Journal of Catalysis*, vol. 305, pp. 307–317, 2013, doi: https://doi.org/10.1016/j.jcat.2013.05.031.

[41] K. Katsiev, G. Harrison, Y. Al-Salik, G. Thornton, and H. Idriss, "Gold Cluster Coverage Effect on H2 Production over Rutile TiO2(110)," *ACS Catalysis*, vol. 9, no. 9, pp. 8294–8305, Sep. 2019, doi: 10.1021/acscatal.9b01890.

[42] V. Vaiano and G. Iervolino, "Photocatalytic Hydrogen Production from Glycerol Aqueous Solution Using Cu-Doped ZnO under Visible Light Irradiation," *Applied Sciences*, vol. 9, no. 13, p. 2741, 2019, doi: 10.3390/app9132741.

[43] Y. Wu, K.-Q. Sun, J. Yu, and B.-Q. Xu, "A key to the storage stability of Au/TiO2 catalyst," *Phys. Chem. Chem. Phys.*, vol. 10, no. 42, pp. 6399–6404, 2008, doi: 10.1039/B807040G.

Annex A – Reaction Network: Glycerol to Hydrogen

The full conversion of glycerol to intermediates and final products is proposed in Figure 18. First, glycerol can be dehydrogenated or dehydrated, or both (in series, also known as hydrogenolysis). Dehydrogenation of glycerol leads to the formation of glyceraldehyde and dihydroxyacetone, that can be hydrogenolyzed to propylene glycol. Dehydration of glycerol leads to the formation of hydroxyacetone and 3-hydroxypropanal. Several other intermediates can be formed upon further dehydration, dehydrogenation and even decarbonylation (C—C cleavage), which reduces the number of carbon atoms in the molecules, until CO_2 and CO are formed. Hydrogen is produced all over this reaction network, as depicted in Figure 18, listing all of the proposed possible mechanisms and consequent intermediary species.

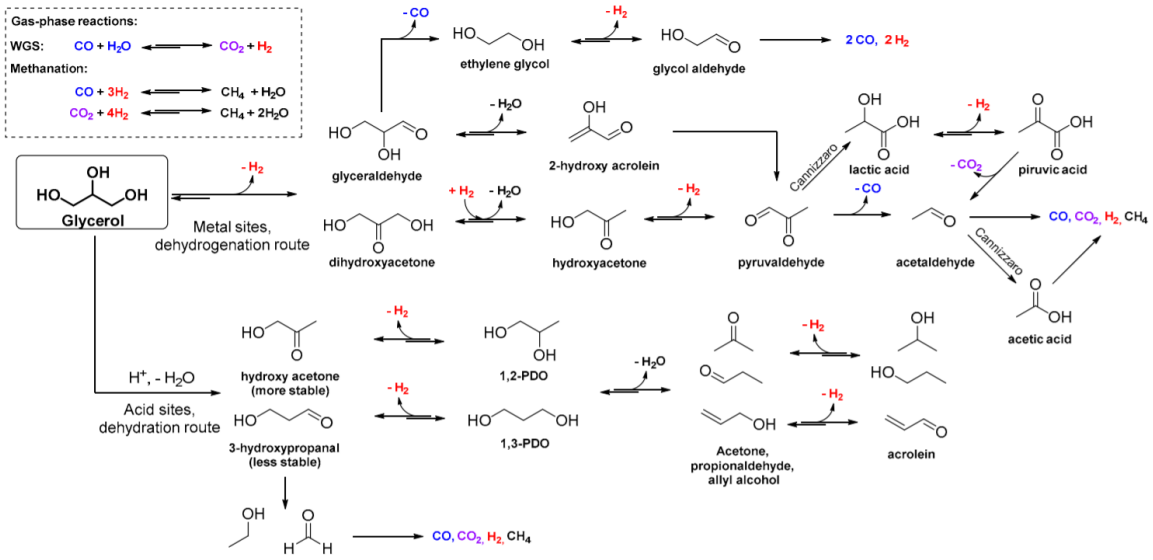

Figure 19 — Reaction network for the glycerol conversion into hydrogen.

Annex B – Point of Zero Charge

The pHpzc, or point of zero charge, was evaluated for a photocatalyst, 3%Au/TiO_2, by preparing two different solutions of 5 different pH values (4, 5, 6, 7 and 8), and adding the catalyst to one of them. They were then put into an agitator, at 84 rotations per minute, to be thoroughly mixed, at a constant rate, for 24 hours. The final pH values were then measured, to compare them with the initial pH values. The pHpzc was determined to be 6.38, as depicted in Figure 19.

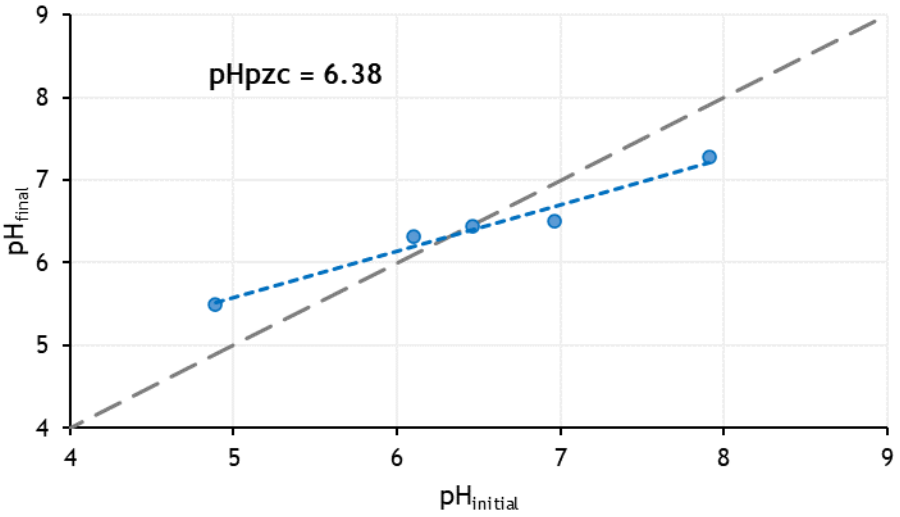

Figure 20 – pHpzc of a 3%Au/TiO_2 photocatalyst.

Annex C – Lamp Spectrum

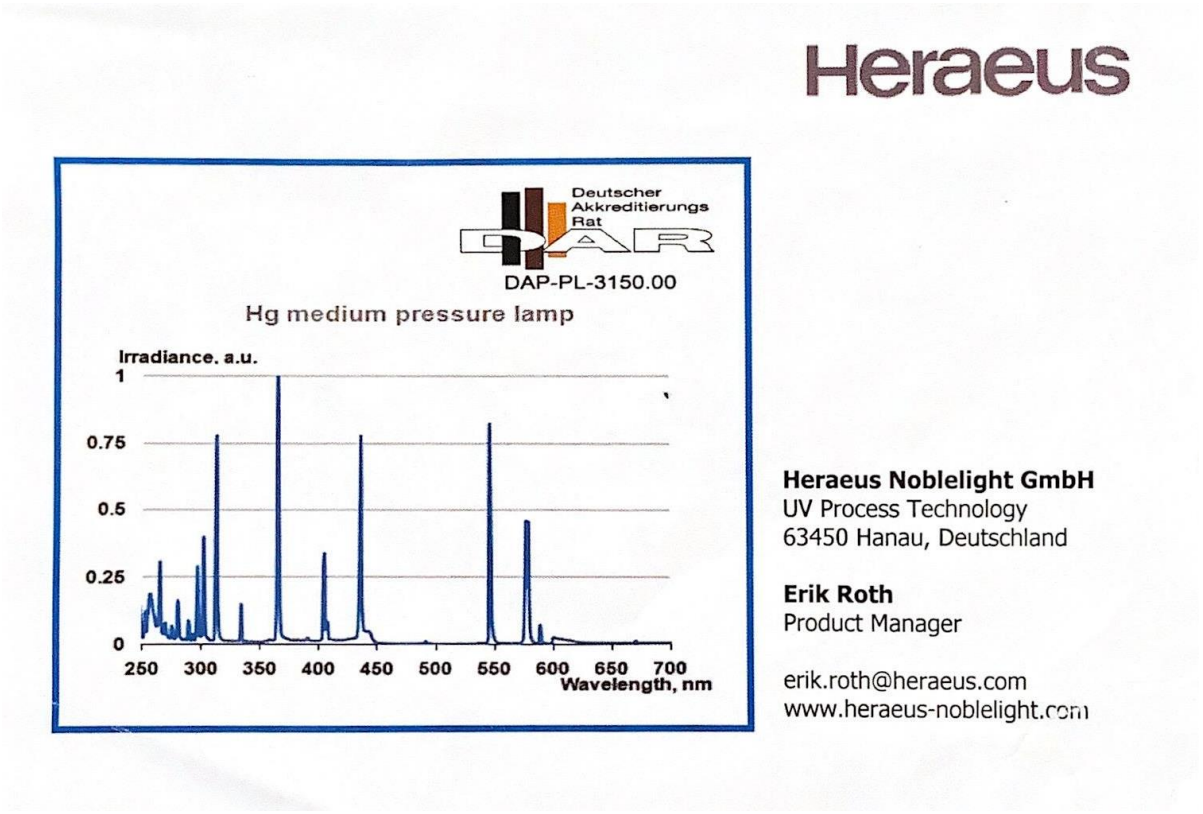

Figure 21 — Spectra of the radiation source (Hg lamp, Heraeus)